Nonlinear Optimal Control for a Gas Compressor Actuated by a Five-Phase Induction Motor

G. Rigatos[1],[*] , M. Abbaszadeh[2], B. Sari[3], P. Siano[4]

[1]Unit of Industrial Automation, Industrial Systems Institute, Rion Patras 26504, Greece
[2]Department of ECS Engineering, Rensselaer Polytechnic Institute, New York 12065, USA
[3]Department of Electrical Engineering, University of Setif I, Setif 19000, Algeria
[4]Department of Innovation Systems, University of Salerno, Fisciano 84084, Italy

Abstract: The article proposes a nonlinear optimal control method for the dynamic model of a gas centrifugal compressor being actuated by a five-phase induction motor (5-phase IM). To achieve high torque and high power in the functioning of gas compressors, 5-phase IM appear to be advantageous in comparison to three-phase synchronous or asynchronous electric machines. The dynamic model of the integrated compression system, which comprises the gas compressor and the 5-phase IM, is first written in a nonlinear and multivariable state-space form. It is proven that the electrically driven gas-compression system is differentially flat. Next, this system is approximately linearised around a temporary operating point that is recomputed at each sampling interval. The linearisation is based on first-order Taylor series expansion and uses the computation of the Jacobian matrices of the state-space model of the integrated system. For the linearised state-space description of the compressor and 5-phase IM, a stabilising optimal (H-infinity) feedback controller is designed. This controller achieves a solution to the nonlinear optimal control problem of the compressor and 5-phase IM system under model uncertainty and external perturbations. The feedback gains of the controller are computed by solving an algebraic Riccati equation at each iteration of the control method. Lyapunov analysis is used to demonstrate global stability for the control loop. Additionally, the H-infinity Kalman filter is used as a robust state estimator, which allows for implementing sensorless control for the gas compression system.

Keywords: gas compressor • five-phase induction motor • nonlinear H-infinity control • global stability • differential flatness properties

1. Introduction

Centrifugal gas compressors are widely used in the natural gas processing industry, as for instance in gas terminals, in the loading or unloading of LNG (Liquified Natural Gas) ships, and in the supply of gas distribution networks with natural gas at the specified pressure levels (Budinis and Thornhill, 2018; Han et al., 2022; Ma et al., 2019; Torissi et al., 2019). Such centrifugal gas compressors are mechanically actuated by gas turbines or by electric motors. In case of electric actuation, synchronous or asynchronous (inductance) three-phase motors are commonly used (Behegen and Gravdahl, 2008; Gravdahl et al., 2002; Torissi et al., 2015). More recently, the use of multiphase motors for the actuation of gas compressors has been also considered (Priestley et al., 2018; Tribelsi and Semail, 2021; Zhou et al., 2019). Multiphase motors have been employed for long in applications where high power and high torque are needed (Echeikh et al., 2016, 2018; Martin et al., 2016). By distributing the required power in a large number of phases, the power load of each individual phase is reduced (Bernudes et al., 2020; Li et al., 2020; Saad et al., 2019). Consequently, the associated power electronics (voltage source converters) function also at smaller voltages and currents. Another feature is that the cumulative rates of power in multiphase machines can be raised without stressing the connected converters (Khadar et al., 2021; Morawiec and Wilczynski, 2022; Morawiec et al., 2020). Furthermore, the frequency of PWM inputs can be increased while the amplitude of such inputs can

be reduced, and this signifies avoidance of mechanical vibrations during the functioning of the motor. Multiphase motors are also fault tolerant because such machines remain functional even if failures affect certain phases (Arahal et al., 2010; Riveros et al., 2018).

Five-phase PM (Permanent Magnet) synchronous motors and five-phase asynchronous induction motors are among the types of multiphase motors one can consider for the actuation of gas compressors (Gonzalez-Prieto et al., 2018; Xiong et al., 2020). For ensuring the reliable performance of such multiphase motors, elaborated nonlinear control methods should be developed (Arahal et al., 2020a, 2020b; Arashloo et al., 2019). To this end, the use of model-predictive control (MPC), backstepping control, and sliding-mode control methods has been proposed (Echeikh et al., 2020; Xiang and Li, 2022). Moreover, fault diagnosis methods for gas compressors have been developed (Lu et al., 2016; Mochammad et al., 2021; Soleymani et al., 2019). In the present article, a novel nonlinear optimal control approach has been developed for an integrated gas compression system that is electrically actuated by a five-phase induction motor (5-phase IM). The dynamic model of the gas compressor and 5-phase IM undergoes first approximate linearisation around the temporary operating point (x^*, u^*) using first-order Taylor series expansion and the computation of the associated Jacobian matrices (Basseville and Nikiforov, 1993; Rigatos and Tzafestas, 2007; Rigatos and Zhang, 2009). The linearisation process takes place at each sampling instance and the linearisation point is defined by the present value of the system's state vector x^* and by the last sampled value of the control inputs vector u^*. The modelling error that is due to the truncation of higher-order terms from the Taylor series is considered to be a perturbation that is asymptotically compensated by the robustness of the control algorithm. For the approximately linearised model of the gas-compression system, a stabilising H-infinity feedback controller is designed. This H-infinity controller achieves the solution of the optimal control problem under model uncertainty and external perturbations.

The proposed optimal (H-infinity) controller represents a min–max differential game taking place between: (i) the control inputs of the gas compression system that try to minimise a cost function containing a quadratic term of the state vector's tracking error; and (ii) the model uncertainty and exogenous perturbation terms that try to maximise this cost function. To select the feedback gains of the H-infinity controller, an algebraic Riccati equation has to be solved repetitively at each time-step of the control method (Rigatos, 2015, 2016; Rigatos and Karapanou, 2020; Rigatos et al., 2022). The global stability properties of the control scheme are proven through Lyapunov analysis. First, it is demonstrated that the control loop of the gas compressor and the 5-phase induction motor satisfies the H-infinity tracking performance criterion. This signifies disturbance rejection and compensation for model uncertainty and exogenous perturbations (Rigatos, 2011; Toussaint et al., 2000). Moreover, under moderate conditions, the global asymptotic stability properties of the control scheme are proven (Rigatos, 2016). The proposed nonlinear optimal control method achieves fast and accurate tracking of reference setpoints under moderate variations of the control inputs. Furthermore, to perform state estimation-based control without the need to measure the entire state vector of the gas-compression system, the H-infinity Kalman filter has been used as a robust state estimator.

The proposed nonlinear optimal control method is novel in comparison to past attempts for solving the optimal control problem for nonlinear dynamical systems (Rigatos, 2015; Rigatos and Karapanou, 2020). Unlike past approaches, in the new nonlinear optimal control method linearisation is performed around a temporary operating point, which is defined by the present value of the system's state vector and by the last sampled value of the control inputs vector and not at points that belong to the desirable trajectory (setpoints). Besides, the Riccati equation, which is used for computing the feedback gains of the controller, is new, and so is the global stability proof for this control method. Compared to nonlinear model-predictive control (NMPC), which is a popular approach for treating the optimal control problem in industry, the new nonlinear optimal (H-infinity) control scheme is of proven global stability and the convergence of its iterative search for the optimum does not depend on initial conditions and trials with multiple sets of controller parameters. It is also noteworthy that the nonlinear optimal control method is applicable to a wider class of dynamical systems than approaches based on the solution of state-dependent Riccati equations (SDRE). The SDRE approaches can be applied only to dynamical systems that can be transformed to the linear parameter varying (LPV) form. Besides, the nonlinear optimal control method performs better than nonlinear optimal control schemes that use approximation of the solution of the Hamilton–Jacobi–Bellman equation by Galerkin series expansions. The stability properties of the optimal control approaches that are based on Galerkin series expansion are still unproven. Finally, it is noted that the article's results have an industrial perspective and the potential for use in industrial applications (Durantay et al., 2019a, 2919b; Singhal, 2014; Tessarolo et al., 2011; Verma et al., 2017).

The structure of the article is as follows: in Section 2, an analysis of the dynamic model of the gas compressor that is actuated by a 5-phase IM is provided. In Section 3, the differential flatness properties of the integrated gas

compression system are proven. In Section 4, the state-space model of the gas-compression system undergoes approximate linearisation using first-order Taylor series expansion and computation of the associated Jacobian matrices. In Section 5, a stabilising H-infinity feedback controller is designed for the dynamic model of the gas-compression system. In Section 6, the stability properties of this control scheme are proven through Lyapunov analysis. Besides, the state estimation problem for the gas compression system is treated with the use of the H-infinity Kalman filter. In Section 7, simulation tests are presented concerning the nonlinear optimal control of the gas-compression system. Finally, in Section 8, concluding remarks are stated.

2. Dynamic Model of the Gas Compressor and 5-phase IM System

The diagram of the gas compressor that is actuated by a 5-phase IM is shown in Figure 1. Through the inlet valve, which is denoted by the gain K_i, the gas is fed into the inlet tank, which is described by pressure variable P_i. Next, the gas passes through the compressor at a mass flow rate, which is denoted as m. The rotational motion of the compressor is due to the torque, which is provided by a 5-phase IM. The angular speed of the compressor and of the 5-phase IM is defined as ω. The gas that comes out of the compressor is stored in the outlet tank, and the pressure at which this storage is maintained is denoted as P_o. In the output of the outlet tank, there is an outlet valve, which is described by gain K_o. Moreover, it is possible to recycle part of the gas of the outlet tank back to the inlet tank, through a valve that is denoted by gain K_r, as mentioned by Torissi et al. (2019).
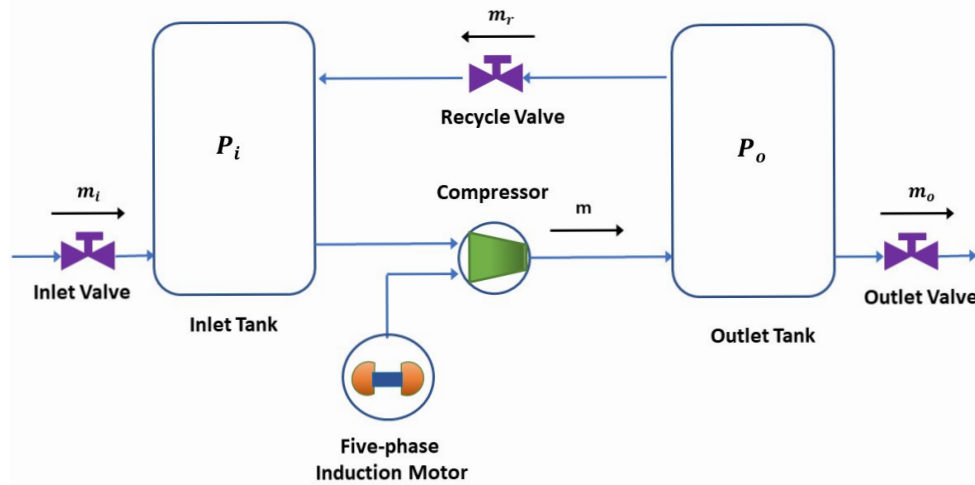

Fig. 1. Diagram of the integrated gas compression system that comprises a centrifugal gas compressor actuated by a 5-phase IM. 5-phase IM, five-phase induction motor. Authors' own work.

The state vector of the compressor is defined as (Torissi et al. [2019]):

$$x = [x_1, x_2, x_3, x_4, x_5]^T = [P_i, P_o, m, w, m_r]^T \tag{1}$$

whereas the state equations of the centrifugal compressor are given by:

$$
\begin{aligned}
\dot{x}_1 &= \tfrac{a_i^2}{V_i}[K_i\sqrt{p_{atm} - x_1} - x_3 + x_5] \\
\dot{x}_2 &= \tfrac{a_o^2}{V_o}[-K_o\sqrt{x_2 - p_{atm}} + x_3 - x_5] \\
\dot{x}_3 &= \tfrac{1}{L}[\pi(x_3, x_4)x_1 - x_2] \\
\dot{x}_4 &= \tfrac{1}{J}[\tau_d - \tau_c(x_3, x_4) - vx_4] \\
\dot{x}_5 &= \tfrac{1}{T_r}[K_r\sqrt{x_2 - x_1} - K_i\sqrt{p_{atm}} - x_1]
\end{aligned}
\tag{2}
$$

The atmospheric pressure is denoted as p_{atm}. The compressor's characteristic function is denoted as $p(x_3, x_4)$ and is taken to be a polynomial function of state variables x_3 and x_4. Equivalently, the compressor's torque is denoted

as $\tau_c(x_3,x_4)$ and is also taken to be a polynomial function of state variables x_3 and x_4. The torque that enables the rotational motion of the compressor is denoted as τ_d and coincides with the electromagnetic torque of the 5-phase IM. The 5-phase IM that is fed by a voltage source inverter is shown in Figure 2.
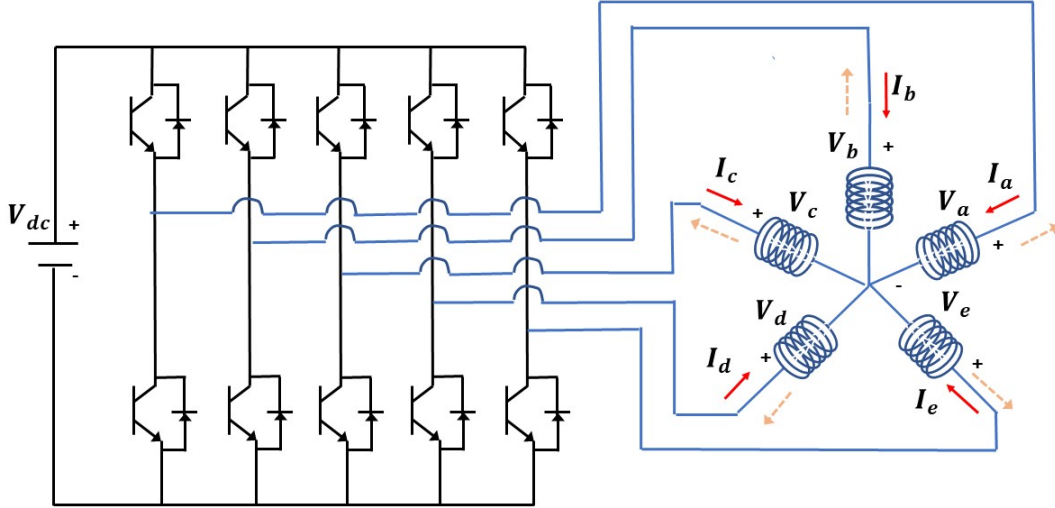

Fig. 2. Diagram of the 5-phase induction motor driven by a voltage source inverter. Authors' own work.

The polynomial approximations of functions $\pi(m,\omega)$ and $\tau(m,\omega)$ are:

(a) $\quad p(x_3,x_4) = (a_0 + a_1 x_3 +$

$\quad a_2 x_3^2 + a_3 x_3^3) \times (b_0 + b_1 x_4 + b_2 x_4^2 + b_3 x_4^3)$, where $a_i, i = 0,1,2,3$ and $b_i, i = 0,1,2,3$ are constants.

(b) $\quad \tau(x_3,x_4) = (c_0 + c_1 x_3 + c_2 x_3^2 + c_3 x_3^3) \times (d_0 + d_1 x_4 + d_2 x_4^2 + d_3 x_4^3)$, where $c_i, i = 0,1,2,3$ and $d_i, i = 0,1,2,3$ are constants.

The state vector of the 5-phase IM is given by Echeikh et al. (2018), Echeikh et al. (2016), and Martin et al. (2016), in terms of the following expression:

$$x = [\omega_r, x_6, x_7, x_8, x_9, x_{10}, x_{11}]^T =$$
$$= [\omega_r, i_{s,a}, i_{s,\beta}, \psi_{r,a}, \psi_{r,\beta}, i_{s,x}, i_{s,y}]^T \tag{3}$$

In this notation, $i_{s,a}, i_{s,\beta}$ and $i_{s,x}, i_{s,y}$ describe the current variables of the stator after applying a generalised Clarke transformation to the five-phase currents vector of the motor. Moreover, $\psi_{r,a}$ and $\psi_{r,\beta}$ are the coefficients of the magnetic flux of the rotor (Echeikh et al., 2016, 2018; Martin et al., 2016). Next, the state equations that describe the dynamics of the 5-phase IM are given to be the following:

$$\dot{\omega}_r = m_1 T_e - m_1 T_L - m_2 \omega_r$$
$$\dot{x}_6 = aA_r x_8 + a\omega r x_9 - bx_6 + cv_{s,a}$$
$$\dot{x}_7 = aA_r x_9 - a\omega r x_8 - bx_7 + cv_{s,b}$$
$$\dot{x}_8 = -A_r x_8 - \omega_r x_9 + MA_r x_6 \tag{4}$$
$$\dot{x}_9 = -A_r x_9 + \omega_r x_8 + MA_r x_7 \, \dot{x}_{10} = dx_{10} + evs, x \, \dot{x}_{11} = dx_{11} + evs, y$$

The electromagnetic torque of the five-phase motor is given by:

$$T_e = \frac{PM}{L_r}(\psi_{r,a} i_{s,b} - \psi_{r,b} i_{s,a}) \Rightarrow$$
$$T_e = \frac{PM}{L_r}(x_8 x_7 - x_9 x_6) \tag{5}$$

The coefficients of the dynamic model of the 5-phase IM are: $a = \frac{M}{\sigma L_s L_r}$, $A_r = \frac{1}{\tau_r}$, $\tau_r = \frac{L_r}{R_r}$,

$$b = \frac{R_s}{\sigma L_s} + \frac{R_r M^2}{\sigma L_s L_r^2}, \, \sigma = 1 - \frac{M^2}{L_s L_r}, \, c = \frac{1}{\sigma L_s}, \, d = -\frac{R_s}{L_{1s}}, \, e = \frac{1}{L_{1s}}, \, m_1 = \frac{P}{J}, \, m_2 = \frac{B_m}{J}.$$

In the above coefficients, R_r and L_r are, respectively, the resistance and the inductance of the rotor, R_s and L_s are, respectively, the resistance and the inductance of the stator, M is the mutual inductance between the stator and the rotor, and L_{1s} is the leakage induction of the stator.

It is noted the above model of the 5-phase induction motors has been based on known reference frames transformations that are used for multiphase electric machines. Thus, using Clarke's transformation for five-phase systems, the 5-phase motor can be described in terms of the couple of two-phase frames ab and xy, where $v = \frac{2\pi}{3}$ (Echeikh et al., 2016; Gonzalez-Prieto et al., 2018).

$$
\begin{pmatrix} v_{s,a} \\ v_{s,b} \\ v_{s,x} \\ v_{s,y} \\ v_{s,0} \end{pmatrix} = \begin{pmatrix} 1 & \cos(v) & \cos(2v) & \cos(3v) & \cos(4v) \\ 0 & \sin(v) & \sin(2v) & \sin(3v) & \sin(4v) \\ 1 & \cos(2v) & \cos(4v) & \cos(v) & \sin(3v) \\ 0 & \sin(2v) & \sin(4v) & \sin(v) & \sin(3v) \\ \frac{1}{\sqrt{2}} & \frac{1}{\sqrt{2}} & \frac{1}{\sqrt{2}} & \frac{1}{\sqrt{2}} & \frac{1}{\sqrt{2}} \end{pmatrix} \begin{pmatrix} v_a \\ v_b \\ v_c \\ v_d \\ v_e \end{pmatrix}
\tag{6}
$$

By connecting the gas compressor with the 5-phase IM, the turn speed of the motor coincides with the one of the compressor, implying that $\omega = \omega_r$. Besides, the torque τ_d that activates the compressor coincides with the electromagnetic torque of the motor, implying that $\tau_d = T_e$. Consequently, it holds that

$$
\tau_d = \frac{PM}{L_r}(x_8 x_7 - x_9 x_6)
\tag{7}
$$

Thus, the integrated model of the gas compression system becomes:

$$
\begin{aligned}
\dot{x}_1 &= \frac{a_i^2}{V_i}[K_i\sqrt{p_{atm} - x_1} - x_3 + x_5] \\
\dot{x}_2 &= \frac{a_o^2}{V_o}[-K_o\sqrt{x_2 - p_{atm}} + x_3 - x_5] \\
\dot{x}_3 &= \frac{1}{L}[\pi(x_3, x_4)x_1 - x_2] \\
\dot{x}_4 &= \frac{1}{J}[\tau_d - \tau_c(x_3, x_4) - vx_4] \\
\dot{x}_5 &= \frac{1}{T_r}[K_r\sqrt{x_2 - x_1} - K_i\sqrt{p_{atm}} - x_1] \\
\dot{x}_6 &= aA_r x_8 + a\omega_r x_9 - bx_6 + cv_{s,a} \\
\dot{x}_7 &= aA_r x_9 - a\omega_r x_8 - bx_7 + cv_{s,b} \\
\dot{x}_8 &= -A_r x_8 - \omega_r x_9 + MA_r x_6 \\
\dot{x}_9 &= -A_r x_9 + \omega_r x_8 + MA_r x_7 \\
\dot{x}_{10} &= dx_{10} + ev_{s,x} \\
\dot{x}_{11} &= dx_{11} + ev_{s,y}
\end{aligned}
\tag{8}
$$

Moreover, using the following notation about the aggregate control inputs vector of the system:

$$
\begin{aligned}
u &= [u_1, u_2, u_3, u_4, u_5, u_6]^T = \\
&= [K_r, K_i, v_{s,a}, v_{s,b}, v_{s,x}, v_{s,y}]^T
\end{aligned}
\tag{9}
$$

the state-space model of the integrated gas compressor and 5-phase IM can be also written in the form

$$
\begin{pmatrix} \dot{x}_1 \\ \dot{x}_2 \\ \dot{x}_3 \\ \dot{x}_4 \\ \dot{x}_5 \\ \dot{x}_6 \\ \dot{x}_7 \\ \dot{x}_8 \\ \dot{x}_9 \\ \dot{x}_{10} \\ \dot{x}_{11} \end{pmatrix} = \begin{pmatrix} \frac{a_i^2}{V_i}(-x_3 + x_5) \\ \frac{a_o^2}{V_o}[-K_o\sqrt{x_2 - p_{atm}} + x_3 - x_5] \\ \frac{1}{L}[\pi(x_3, x_4)x_1 - x_2] \\ \frac{1}{J}[\tau_d - \tau_c(x_3, x_4) - vx_4] \\ 0 \\ aA_r x_8 + a\omega_r x_9 - bx_6 \\ aA_r x_9 - a\omega_r x_8 - bx_7 \\ -A_r x_8 - \omega_r x_9 + MA_r x_6 \\ -A_r x_9 + \omega_r x_8 + MA_r x_7 \\ dx_{10} \\ dx_{11} \end{pmatrix} + \begin{pmatrix} \frac{a_i^2}{V_i}\sqrt{p_{atm} - x_1} & 0 & 0 & 0 & 0 & 0 \\ 0 & 0 & 0 & 0 & 0 & 0 \\ 0 & 0 & 0 & 0 & 0 & 0 \\ 0 & 0 & 0 & 0 & 0 & 0 \\ -\frac{1}{T_r}\sqrt{p_{atm} - x_1} & \frac{1}{T_r}\sqrt{x_2 - x_1} & 0 & 0 & 0 & 0 \\ 0 & 0 & c & 0 & 0 & 0 \\ 0 & 0 & 0 & c & 0 & 0 \\ 0 & 0 & 0 & 0 & 0 & 0 \\ 0 & 0 & 0 & 0 & 0 & 0 \\ 0 & 0 & 0 & 0 & e & 0 \\ 0 & 0 & 0 & 0 & 0 & e \end{pmatrix} \begin{pmatrix} u_1 \\ u_2 \\ u_3 \\ u_4 \\ u_5 \\ u_6 \end{pmatrix}
\tag{10}
$$

The integrated system can be also written in the nonlinear affine-in-the-input state-space form

$$\dot{x} = f(x) + g(x)u \tag{11}$$

where $x \in R^{11 \times 1}$, $f(x) \in R^{11 \times 1}$, $g(x) \in R^{11 \times 6}$, and $u \in R^{6 \times 1}$.

3. Differential Flatness Properties of the Integrated Gas-Compression System

It will be proven that the integrated gas-compression system that consists of a gas compressor serially connected to a 5-phase IM is differentially flat. The differential flatness property signifies that all state variables and the control inputs of the system are differential functions of its flat outputs. The flat outputs of the system are:

$$Y = [y_1, y_2, y_3, y_4, y_5, y_6]^T \Rightarrow Y = [x_1, x_4, x_8, x_9, x_{10}, x_{11}]^T \tag{12}$$

From the eighth row of the state-space model of Eq. (10), one solves for x_6. It holds that

$$\dot{x}_8 = -A_r x_8 - x_4 x_9 + MA_r x_6 \Rightarrow x_6 = \frac{\dot{x}_8 + A_r x_8 + x_4 x_9}{MA_r}$$
$$\Rightarrow x_6 = h_6(Y, \dot{Y}) \tag{13}$$

which signifies that x_6 is a differential function of the flat outputs of the system. Next, from the ninth row of the state-space model of Eq. (10) one solves for x_7. This gives

$$\dot{x}_9 = -A_r x_9 - x_4 x_8 + MA_r x_7 \Rightarrow x_7 = \frac{\dot{x}_9 + A_r x_9 - x_4 x_8}{MA_r}$$
$$\Rightarrow x_7 = h_7(Y, \dot{Y}) \tag{14}$$

which signifies that x_7 is a differential function of the flat outputs of the system. Next, from the sixth row of the state-space model of Eq. (10) one solves for u_3. It holds that

$$\dot{x}_6 = aA_r x_8 + ax_4 x_9 - bx_6 + cu_3 \Rightarrow u_3 = \frac{\dot{x}_6 - aA_r x_8 - ax_4 x_9 + bx_6}{c}$$
$$\Rightarrow u_3 = h_{u_3}(Y, \dot{Y}) \tag{15}$$

which signifies that u_3 is a differential function of the flat outputs of the system. Moreover, from the seventh row of the state-space model of Eq. (10), one solves for u_4. This gives

$$\dot{x}_7 = aA_r x_9 - ax_4 x_8 - bx_7 + cu_4 \Rightarrow u_3 = \frac{\dot{x}_7 - aA_r x_9 + ax_4 x_8 + bx_7}{c}$$
$$\Rightarrow u_4 = h_{u_4}(Y, \dot{Y}) \tag{16}$$

which signifies that u_4 is a differential function of the flat outputs of the system. Additionally, from the 10th row of the state-space model of Eq. (10), one solves for u_5. This gives

$$\dot{x}_{10} = dx_{10} + eu_5 \Rightarrow u_5 = \frac{\dot{x}_{10} - dx_{10}}{e}$$
$$\Rightarrow u_5 = h_{u_5}(Y, \dot{Y}) \tag{17}$$

which signifies that u_5 is a differential function of the flat outputs of the system. Furthermore, from the 11th row of the state-space model of Eq. (10), one solves for u_6. This gives

$$\dot{x}_{11} = dx_{11} + eu_5 \Rightarrow u_6 = \frac{\dot{x}_{11} - dx_{11}}{e}$$
$$\Rightarrow u_6 = h_{u_6}(Y, \dot{Y}) \tag{18}$$

Additionally, from the fourth row of the state-space model of Eq. (10), one solves for x_3. This gives

$$\dot{x}_4 = \tfrac{1}{J}[\tau_d - \tau_c(x_3, x_4) - vx_4] \Rightarrow \tau_c(x_3, x_4) = -J\dot{x}_4 + \tfrac{PM}{L_r}(x_8 x_7 - x_9 x_6) - vx_4$$
$$\Rightarrow x_3 = h_3(Y, \dot{Y}) \tag{19}$$

where it has been used that $\tau(x_3, x_4)$ is a polynomial function of x_3 and x_4, for instance $\tau(x_3, x_4) =$

$$(c_0 + c_1 x_3 + c_2 x_3^2 + c_3 x_3^3) \times (d_0 + d_1 x_4 + d_2 x_4^2 + d_3 x_4^3).$$

Thus, the first row of Eq. (19) gives a polynomial function of x_3 and as a consequence the second row of Eq. (19) shows that x_3 is a differential function of the flat outputs of the system.

Next, from the third row of the state-space model of Eq. (10), one solves for x_2. This gives

$$\dot{x}_3 = \tfrac{1}{L}[\pi(x_3, x_4)x_1 - x_2] \Rightarrow x_2 = -L\dot{x}_3 + \pi(x_3, x_4)x_1$$
$$\Rightarrow x_2 = h_2(Y, \dot{Y}) \tag{20}$$

which signifies that x_2 is a differential function of the flat outputs. Moreover, from the third row of the state-space model of Eq. (10), one solves for x_5. This gives

$$\dot{x}_2 = \tfrac{a_o^2}{V_o}[-K_o\sqrt{x_2 - p_{atm}} + x_3 - x_5] \Rightarrow x_5 = -\tfrac{V_o}{a_o^2}\dot{x}_2 - K_o\sqrt{x_2 - p_{atm}}$$
$$\Rightarrow x_5 = h_5(Y, \dot{Y}) \tag{21}$$

which signifies that x_5 is a differential function of the flat outputs. Furthermore, from the first row of the state-space model of Eq. (10), one solves for u_1. This gives

$$\dot{x}_1 = \tfrac{a_u^2}{V_i}[u_1\sqrt{p_{atm} - x_1} - x_3 + x_5] \Rightarrow u_1 = \frac{\frac{V_i}{a_i^2}\dot{x}_1 - x_3 + x_5}{\sqrt{p_{atm} - x_1}}$$
$$\Rightarrow u_1 = h_{u_1}(Y, \dot{Y}) \tag{22}$$

which signifies that u_1 is a differential function of the flat outputs. Additionally, from the fifth row of the state-space model of Eq. (10), one solves for u_2. This gives

$$\dot{x}_5 = \tfrac{1}{T_r}[u_2\sqrt{x_2 - x_1} - u_1\sqrt{p_{atm} - x_1}] \Rightarrow u_2 = \frac{T_r\dot{x}_5 + u_1\sqrt{p_{atm} - x_1}}{\sqrt{x_2 - x_1}}$$
$$\Rightarrow u_2 = h_{u_2}(Y, \dot{Y}) \tag{23}$$

which signifies that u_2 is a differential function of the flat outputs. According to the previous analysis, all state variables and the control inputs of the integrated system that comprise a gas compressor actuated by a 5-phase IM can be expressed as differential functions of the system's flat outputs. Consequently, the entire system is differentially flat.

The differential flatness property is an implicit proof of the system's controllability and allows also for computing feasible setpoints for all state variables of the system. First, one selects setpoints for the flat outputs of the gas compression system $x_1, x_4, x_8, x_9, x_{10}, x_{11}$ in an unconstrained manner. Next, setpoints are selected for the rest of the state vector elements x_2, x_3, x_5, x_6, x_7 under the constraint that these state variables are differential functions of the flat outputs.

4. Approximate Linearisation of the Dynamic Model of the Gas-Compression System

The dynamic model of the gas-compression system undergoes approximate linearisation around the temporary operating point (x^*, u^*), where x^* is the present value of the system's state vector and u^* is the last sampled value of the control inputs vector. The linearisation takes place at each sampling instance and is based on first-order Taylor series expansion. The modelling error that is due to truncation of higher-order terms from the Taylor series is viewed as a perturbation that is asymptotically compensated by the robustness of the control algorithm.

The initial nonlinear model of the gas-compression system is in the nonlinear affine-in-the-input state-space form:

$$\dot{x} = f(x) + g(x)u \; x \in R^{11 \times 1}, \; f(x) \in R^{11 \times 1}, \; g(x) \in R^{11 \times 6}, \; u \in R^{6 \times 1} \tag{24}$$

After linearisation with the use of a first-order Taylor series expansion, it is written in the equivalent linearised form

$$\dot{x} = Ax + Bu + \tilde{d} \tag{25}$$

where $\tilde{d}$ is the cumulative disturbances vector, which may comprise: (i) the modelling error due to truncation of higher-order terms from the Taylor series, (ii) exogenous perturbations, and (iii) sensor measurement noise of any distribution. Matrices A and B are the Jacobian matrices of the system, which are given by

$$A = \nabla_x[f(x) + g(x)u] \mid_{(x^*, u^*)} \Rightarrow A = \nabla_x[f(x)] \mid_{(x^*, u^*)} + \nabla_x[g_1(x)u] \mid_{(x^*, u^*)} + \nabla_x[g_2(x)u] \mid_{(x^*, u^*)} +$$

$$+ \nabla x[g_3(x)u] \mid_{(x^*, u^*)} + \nabla x[g_4(x)u] \mid_{(x^*, u^*)} + \nabla x[g_5(x)u] \mid_{(x^*, u^*)} + \nabla x[g_6(x)u] \mid_{(x^*, u^*)} \tag{26}$$

$$B = \nabla_u[f(x) + g(x)u] \mid_{(x^*, u^*)} \Rightarrow B = g(x) \mid_{(x^*, u^*)} \tag{27}$$

where $g_i(x)$, $i = 1, 2, \cdots, 6$ are the column vectors that constitute the control inputs gain matrix $g(x) = [g_1(x), g_2(x), g_3(x), g_4(x), g_5(x), g_6(x)]^T$.

This linearisation approach that has been followed for implementing the nonlinear optimal control scheme results into a quite accurate model of the system's dynamics. Consider for instance the following affine-in-the-input state-space model:

$$\dot{x} = f(x) + g(x)u \Rightarrow$$

$$\dot{x} = [f(x^*) + \nabla_x f(x) \mid_{x^*} (x - x^*)] + [g(x^*) + \nabla_x g(x) \mid_{x^*} (x - x^*)]u^* + g(x^*)u^* + g(x^*)(u - u^*) + \tilde{d}_1 \Rightarrow$$

$$\dot{x} = [\nabla_x f(x) \mid_{x^*} + \nabla_x g(x) \mid_{x^*} u^*]x + g(x^*)u - [\nabla_x f(x) \mid_{x^*} + \nabla_x g(x) \mid_{x^*} u^*]x^* + f(x^*) + g(x^*)u^* + \tilde{d}_1 \tag{28}$$

where $\tilde{d}_1$ is the modelling error due to truncation of higher-order terms in the Taylor series expansion of $f(x)$ and $g(x)$. Next, by defining $A = [\nabla_x f(x) \mid_{x^*} + \nabla_x g(x) \mid_{x^*} u^*]$, $B = g(x^*)$ one obtains

$$\dot{x} = Ax + Bu - Ax^* + f(x^*) + g(x^*)u^* + \tilde{d}_1 \tag{29}$$

Moreover, by denoting $\tilde{d} = -Ax^* + f(x^*) + g(x^*)u^* + \tilde{d}_1$ about the cumulative modelling error term in the Taylor series expansion procedure, one has

$$\dot{x} = Ax + Bu + \tilde{d} \tag{30}$$

which is the approximately linearised model of the dynamics of the system of Eq. (25). The term $f(x^*) + g(x^*)u^*$ is the derivative of the state vector at (x_*, u_*), which is almost annihilated by $-Ax^*$.

Next, the elements of the Jacobian matrices are computed. First, the computation of the Jacobian matrix $\nabla_x[f(x)] \mid_{(x^*, u^*)}$ is performed.

First row of the Jacobian matrix $\nabla_x[f(x)] \mid_{(x^*, u^*)}$: $\frac{\partial f_1}{\partial x_1} = 0$, $\frac{\partial f_1}{\partial x_2} = 0$, $\frac{\partial f_1}{\partial x_3} = -\frac{a_i^2}{V_i}$, $\frac{\partial f_1}{\partial x_4} = 0$, $\frac{\partial f_1}{\partial x_5} = \frac{a_i^2}{V_i}$,

$\frac{\partial f_1}{\partial x_6} = 0$, $\frac{\partial f_1}{\partial x_7} = 0$, $\frac{\partial f_1}{\partial x_8} = 0$, $\frac{\partial f_1}{\partial x_9} = 0$, $\frac{\partial f_1}{\partial x_{10}} = 0$, $\frac{\partial f_1}{\partial x_{11}} = 0$.

Second row of the Jacobian matrix $\nabla_x[f(x)] \mid_{(x^*, u^*)}$: $\frac{\partial f_2}{\partial x_1} = 0$, $\frac{\partial f_2}{\partial x_2} = \frac{a_o * 2}{V_o}\left(-\frac{K_o}{2}\right)(x_2 - p_{atm})^{-\frac{1}{2}}$, $\frac{\partial f_2}{\partial x_3} = \frac{a_o^2}{V_o}$,

203

$$\frac{\partial f_2}{\partial x_4} = 0,\ \frac{\partial f_2}{\partial x_5} = 0,\ \frac{\partial f_2}{\partial x_6} = -\frac{a_o^2}{V_o},\ \frac{\partial f_2}{\partial x_7} = 0,\ \frac{\partial f_2}{\partial x_8} = 0,\ \frac{\partial f_2}{\partial x_9} = 0,\ \frac{\partial f_2}{\partial x_{10}} = 0,\ \frac{\partial f_2}{\partial x_{11}} = 0.$$

Third row of the Jacobian matrix $\nabla_x[f(x)]\mid_{(x^*,u^*)}$: $\frac{\partial f_3}{\partial x_1} = \frac{1}{L}\pi(x_3,x_4),\ \frac{\partial f_3}{\partial x_2} = -\frac{1}{L},\ \frac{\partial f_3}{\partial x_3} = \frac{1}{L}\frac{\partial\pi(x_3,x_4)}{\partial x_3}x_1,$

$$\frac{\partial f_3}{\partial x_4} = \frac{1}{L}\frac{\partial\pi(x_3,x_4)}{\partial x_4}x_1,\ \frac{\partial f_3}{\partial x_5} = 0,\ \frac{\partial f_3}{\partial x_6} = 0,\ \frac{\partial f_3}{\partial x_7} = 0,\ \frac{\partial f_3}{\partial x_8} = 0,\ \frac{\partial f_3}{\partial x_9} = 0,\ \frac{\partial f_3}{\partial x_{10}} = 0,\ \frac{\partial f_3}{\partial x_{11}} = 0.$$

where using that $\pi(x_3,x_4) = (a_0 + a_1 x_3 + a_2 x_3^2 + a_3 x_3^3)\times(b_0 + b_1 x_4 + b_2 x_4^2 + b_3 x_4^3)$ it holds that

$$\frac{\partial\pi(x_3,x_4)}{\partial x_3} = (a_1 + 2a_2 x_3 + 3a_3 x_3^2)\times(b_0 + b_1 x_4 + b_2 x_4^2 + b_3 x_4^3)$$

$$\frac{\partial\pi(x_3,x_4)}{\partial x_4} = (a_0 + a_1 x_3 + a_2 x_3^2 + a_3 x_3^3)\times(b_1 + 2b_2 x_4 + 3b_3 x_4^2)$$

Fourth row of the Jacobian matrix $\nabla_x[f(x)]\mid_{(x^*,u^*)}$: $\frac{\partial f_4}{\partial x_1} = 0,\ \frac{\partial f_4}{\partial x_2} = 0,\ \frac{\partial f_4}{\partial x_3} = -\frac{1}{J}\frac{\partial\tau_c(x_3,x_4)}{\partial x_3},\ \frac{\partial f_4}{\partial x_4} =$

$\frac{1}{J}\frac{\partial\tau_c(x_3,x_4)}{\partial x_3},\ \frac{\partial f_4}{\partial x_5} = 0,\ \frac{\partial f_4}{\partial x_6} = -\frac{1}{J}\frac{PM}{L_r}x_9,\ \frac{\partial f_4}{\partial x_7} = \frac{1}{J}\frac{PM}{L_r}x_8,\ \frac{\partial f_4}{\partial x_8} = \frac{1}{J}\frac{PM}{L_r}x_7,\ \frac{\partial f_4}{\partial x_9} = -\frac{1}{J}\frac{PM}{L_r}x_6,\ \frac{\partial f_4}{\partial x_{10}}$ $\frac{\partial f_4}{\partial x_{11}} = 0.$

where using that $\tau_c(x_3,x_4) = (c_0 + c_1 x_3 + c_2 x_3^2 + c_3 x_3^3)\times(d_0 + d_1 x_4 + d_2 x_4^2 + d_3 x_4^3)$ it holds that

$$\frac{\partial\tau_c(x_3,x_4)}{\partial x_3} = (c_1 + 2c_2 x_3 + 3c_3 x_3^2)\times(d_0 + d_1 x_4 + d_2 x_4^2 + d_3 x_4^3)$$

$$\frac{\partial\tau_c(x_3,x_4)}{\partial x_4} = (c_0 + c_1 x_3 + c_2 x_3^2 + c_3 x_3^3)\times(d_1 + 2d_2 x_4 + 3d_3 x_4^2)$$

Fifth row of the Jacobian matrix $\nabla_x[f(x)]\mid_{(x^*,u^*)}$: $\frac{\partial f_5}{\partial x_i} = 0$ for $i = 1, 2, \cdots, 11$

Sixth row of the Jacobian matrix $\nabla_x[f(x)]\mid_{(x^*,u^*)}$: $\frac{\partial f_6}{\partial x_1} = 0,\ \frac{\partial f_6}{\partial x_2} = 0,\ \frac{\partial f_6}{\partial x_3} = 0,\ \frac{\partial f_6}{\partial x_4} = ax_3,\ \frac{\partial f_6}{\partial x_5} = 0,$

$$\frac{\partial f_6}{\partial x_6} = -b,\ \frac{\partial f_6}{\partial x_7} = 0,\ \frac{\partial f_6}{\partial x_8} = aA_r,\ \frac{\partial f_6}{\partial x_9} = ax_4,\ \frac{\partial f_2}{\partial x_{10}} = 0,\ \frac{\partial f_2}{\partial x_{11}} = 0.$$

Seventh row of the Jacobian matrix $\nabla_x[f(x)]\mid_{(x^*,u^*)}$: $\frac{\partial f_7}{\partial x_1} = 0,\ \frac{\partial f_7}{\partial x_2} = 0,\ \frac{\partial f_7}{\partial x_3} = 0,\ \frac{\partial f_7}{\partial x_4} = -ax_4,\ \frac{\partial f_7}{\partial x_5} = 0,$

$$\frac{\partial f_7}{\partial x_6} = 0,\ \frac{\partial f_7}{\partial x_7} = -b,\ \frac{\partial f_7}{\partial x_8} = -ax_4,\ \frac{\partial f_8}{\partial x_9} = aA_r,\ \frac{\partial f_7}{\partial x_{10}} = 0,\ \frac{\partial f_7}{\partial x_{11}} = 0.$$

Eighth row of the Jacobian matrix $\nabla_x[f(x)]\mid_{(x^*,u^*)}$: $\frac{\partial f_8}{\partial x_1} = 0,\ \frac{\partial f_8}{\partial x_2} = 0,\ \frac{\partial f_8}{\partial x_3} = 0,\ \frac{\partial f_8}{\partial x_4} = -x_9,\ \frac{\partial f_8}{\partial x_5} = 0,$

$$\frac{\partial f_8}{\partial x_6} = MA_r,\ \frac{\partial f_8}{\partial x_7} = 0,\ \frac{\partial f_8}{\partial x_8} = -A_r,\ \frac{\partial f_8}{\partial x_9} = -x_4,\ \frac{\partial f_8}{\partial x_{10}} = 0,\ \frac{\partial f_8}{\partial x_{11}} = 0.$$

Ninth row of the Jacobian matrix $\nabla_x[f(x)]\mid_{(x^*,u^*)}$: $\frac{\partial f_9}{\partial x_1} = 0,\ \frac{\partial f_9}{\partial x_2} = 0,\ \frac{\partial f_9}{\partial x_3} = 0,\ \frac{\partial f_9}{\partial x_4} = x_8,\ \frac{\partial f_9}{\partial x_5} = 0,$

$$\frac{\partial f_9}{\partial x_6} = 0,\ \frac{\partial f_9}{\partial x_7} = MA_r,\ \frac{\partial f_9}{\partial x_8} = x_4,\ \frac{\partial f_9}{\partial x_9} = -A_r,\ \frac{\partial f_9}{\partial x_{10}} = 0,\ \frac{\partial f_9}{\partial x_{11}} = 0.$$

Tenth row of the Jacobian matrix $\nabla_x[f(x)]\mid_{(x^*,u^*)}$: $\frac{\partial f_{10}}{\partial x_i} = 0$, for $i \neq 10$, and $\frac{\partial f_{10}}{\partial x_{10}} = d.$

Eleventh row of the Jacobian matrix $\nabla_x[f(x)]\mid_{(x^*,u^*)}$: $\frac{\partial f_{11}}{\partial x_i} = 0$, for $i \neq 11$, and $\frac{\partial f_{11}}{\partial x_{11}} = d.$

Computation of the Jacobian matrix $\nabla_x g_1(x)\mid_{(x^*,u^*)}$.

$$\nabla_x g_1(x)\,|_{(x^*,u^*)} = \begin{pmatrix} -\frac{a_i^2}{2V_i}(p_{atm}-x_1)^{-\frac{1}{2}} & 0 & 0 & 0 & 0 & 0 & 0 & 0 & 0 & 0 & 0 \\ 0 & 0 & 0 & 0 & 0 & 0 & 0 & 0 & 0 & 0 & 0 \\ 0 & 0 & 0 & 0 & 0 & 0 & 0 & 0 & 0 & 0 & 0 \\ 0 & 0 & 0 & 0 & 0 & 0 & 0 & 0 & 0 & 0 & 0 \\ -\frac{1}{2T_r}(p_{atm}-x_1)^{-\frac{1}{2}} & 0 & 0 & 0 & 0 & 0 & 0 & 0 & 0 & 0 & 0 \\ 0 & 0 & 0 & 0 & 0 & 0 & 0 & 0 & 0 & 0 & 0 \\ 0 & 0 & 0 & 0 & 0 & 0 & 0 & 0 & 0 & 0 & 0 \\ 0 & 0 & 0 & 0 & 0 & 0 & 0 & 0 & 0 & 0 & 0 \\ 0 & 0 & 0 & 0 & 0 & 0 & 0 & 0 & 0 & 0 & 0 \\ 0 & 0 & 0 & 0 & 0 & 0 & 0 & 0 & 0 & 0 & 0 \\ 0 & 0 & 0 & 0 & 0 & 0 & 0 & 0 & 0 & 0 & 0 \end{pmatrix} \tag{31}$$

Computation of the Jacobian matrix $\nabla_x g_2(x)\,|_{(x^*,u^*)}$.

$$\nabla_x g_2(x)\,|_{(x^*,u^*)} = \begin{pmatrix} 0 & 0 & 0 & 0 & 0 & 0 & 0 & 0 & 0 & 0 & 0 \\ 0 & 0 & 0 & 0 & 0 & 0 & 0 & 0 & 0 & 0 & 0 \\ 0 & 0 & 0 & 0 & 0 & 0 & 0 & 0 & 0 & 0 & 0 \\ 0 & 0 & 0 & 0 & 0 & 0 & 0 & 0 & 0 & 0 & 0 \\ -\frac{1}{2T_r}(x_2-x_1)^{-\frac{1}{2}} & \frac{1}{2T_r}(x_2-x_1)^{-\frac{1}{2}} & 0 & 0 & 0 & 0 & 0 & 0 & 0 & 0 & 0 \\ 0 & 0 & 0 & 0 & 0 & 0 & 0 & 0 & 0 & 0 & 0 \\ 0 & 0 & 0 & 0 & 0 & 0 & 0 & 0 & 0 & 0 & 0 \\ 0 & 0 & 0 & 0 & 0 & 0 & 0 & 0 & 0 & 0 & 0 \\ 0 & 0 & 0 & 0 & 0 & 0 & 0 & 0 & 0 & 0 & 0 \\ 0 & 0 & 0 & 0 & 0 & 0 & 0 & 0 & 0 & 0 & 0 \\ 0 & 0 & 0 & 0 & 0 & 0 & 0 & 0 & 0 & 0 & 0 \end{pmatrix} \tag{32}$$

Besides, for the rest of the Jacobian matrices of the columns of the control inputs gain matrix $g(x)$, it holds that

$$\nabla_x g_3(x)\,|_{(x^*,u^*)} = 0 \in R^{11\times11} \quad \nabla_x g_4(x)\,|_{(x^*,u^*)} = 0 \in R^{11\times11}$$
$$\nabla_x g_5(x)\,|_{(x^*,u^*)} = 0 \in R^{11\times11} \quad \nabla_x g_6(x)\,|_{(x^*,u^*)} = 0 \in R^{11\times11} \tag{33}$$

5. Design of an H-Infinity Nonlinear Feedback Controller

5.1. Equivalent linearised dynamics of the 5-phase induction motor-driven gas compressor

After linearisation around its current operating point, the dynamic model for the gas compressor that is actuated by a 5-phase IM is written as (Rigatos [2016], Rigatos and Karapanou [2020]):

$$\dot{x} = Ax + Bu + d_1 \tag{34}$$

where parameter d_1 stands for the linearisation error in the model of the integrated system of the gas compressor and the 5-phase IM that was given previously in Eq. (25).

The reference setpoints for the state vector of the aforementioned dynamic model are denoted by $\mathbf{x}_d = [x_1^d, \cdots, x_{11}^d]$. Tracking of this trajectory is achieved after applying the control input u^*. At every time-instant, the control input u^* is assumed to differ from the control input u appearing in Eq. (34) by an amount equal to Δu, as can be expressed in the following form:

$$u^* = u + \Delta u$$
$$\dot{x}_d = Ax_d + Bu^* + d_2 \tag{35}$$

The dynamics of the controlled system described in Eq. (34) can be also written as

$$\dot{x} = Ax + Bu + Bu^* - Bu^* + d_1 \tag{36}$$

and by denoting $d_3 = -Bu^* + d_1$ as an aggregate disturbance term one obtains

$$\dot{x} = Ax + Bu + Bu^* + d_3 \tag{37}$$

By subtracting Eq. (35) from Eq. (37) one has

$$\dot{x} - \dot{x}_d = A(x - x_d) + Bu + d_3 - d_2 \tag{38}$$

By denoting the tracking error as $e = x - x_d$ and the aggregate disturbance term as $\tilde{d} = d_3 - d_2$, the tracking error dynamics becomes

$$\dot{e} = Ae + Bu + \tilde{d} \tag{39}$$

The above linearised form of the model of the gas compressor that is actuated by the 5-phase IM can be efficiently controlled after applying an H-infinity feedback control scheme.

5.2. The nonlinear H-infinity control

The initial nonlinear model of the system gas compressor that is actuated by the 5-phase IM is in the form

$$\dot{x} = f(x,u) \; x \in R^n, \; u \in R^m \tag{40}$$

Linearisation of the model of the integrated system of the gas compressor and 5-phase IM is performed at each iteration of the control algorithm around its present operating point $(x^*,u^*) = (x(t),u(t - T_s))$. The linearised equivalent of the system is described by

$$\dot{x} = Ax + Bu + L\tilde{d} \;\; x \in R^n, \; u \in R^m, \; \tilde{d} \in R^q \tag{41}$$

where matrices A and B are obtained from the computation of the previously defined Jacobians and vector $\tilde{d}$ denotes disturbance terms due to linearisation errors. The problem of disturbance rejection for the linearised model that is described by

$$\dot{x} = Ax + Bu + L\tilde{d} \text{ and } y = Cx, \tag{42}$$

where $x \in R^n$, $u \in R^m$, $\tilde{d} \in R^q$, and $y \in R^p$, cannot be handled efficiently if the classical LQR (Linear Quadratic Regulator) control scheme is applied. This is because of the existence of the perturbation term $\tilde{d}$. The disturbance term $\tilde{d}$, apart from modelling (parametric) uncertainty and external perturbation terms, can also represent noise terms of any distribution.

In the H_∞ control approach, a feedback control scheme is designed for setpoint tracking by the system's state vector and simultaneous disturbance rejection, considering that the disturbance affects the system in the worst possible manner. The disturbances' effects are incorporated in the following quadratic cost function (Rigatos, 2016; Rigatos and Karapanou, 2020):

$$J(t) = \tfrac{1}{2}\int_0^T [y^T(t)y(t) + ru^T(t)u(t) - \rho^2 \tilde{d}^T(t)\tilde{d}(t)]dt, \quad r, \rho > 0 \tag{43}$$

The significance of the negative sign in the cost function's term that is associated with the perturbation variable $\tilde{d}(t)$ is that the disturbance tries to maximise the cost function $J(t)$ whereas the control signal $u(t)$ tries to minimise it. The physical meaning of the relation given above is that the control signal and the disturbances compete to each other within a min–max differential game. This problem of min–max optimisation can be written as $min_u max_{\tilde{d}} J(u,\tilde{d})$.

The objective of the optimisation procedure is to compute a control signal $u(t)$, which can compensate for the worst possible disturbance, that is externally imposed to the system of the gas compressor that is actuated by the 5-phase

IM. However, the solution to the min–max optimisation problem is directly related to the value of the parameter ρ. This means that there is an upper bound in the disturbances magnitude that can be annihilated by the control signal.

5.3. Computation of the feedback control gains

For the linearised system given by Eq. (42) the cost function of Eq. (43) is defined, where coefficient r determines the penalisation of the control input and weight coefficient ρ determines the reward of the disturbances' effects. It is assumed that: (i) the energy that is transferred from the disturbances signal $\tilde{d}(t)$ is bounded, that is $\int_0^\infty \tilde{d}^T(t)\tilde{d}(t)dt < \infty$, (ii) matrices $[A,B]$ and $[A,L]$ are stabilisable, and (iii) matrix $[A,C]$ is detectable. In the case of a tracking problem the optimal feedback control law is given by (Rigatos, 2016; Rigatos and Karapanou, 2020)

$$u(t) = -Ke(t) \tag{44}$$

with $e = x - x_d$ considered as the tracking error, and $K = \frac{1}{r}B^T P$ where P is a positive definite symmetric matrix. As it will be proven in Section 6, matrix P is obtained from the solution of the Riccati equation

$$A^T P + PA + Q - P(\tfrac{2}{r}BB^T - \tfrac{1}{\rho^2}LL^T)P = 0 \tag{45}$$

where Q is a positive semi-definite symmetric matrix. The worst case disturbance is given by

$$\tilde{d}(t) = \tfrac{1}{\rho^2}L^T Pe(t) \tag{46}$$

The solution of the H-infinity feedback control problem for the system of the gas compressor that is actuated by the 5-phase IM and the computation of the worst case disturbance that the related controller can sustain, comes from superposition of Bellman's optimality principle when considering that the compression system is affected by two separate inputs: (i) the control input u and (ii) the cumulative disturbance input $\tilde{d}(t)$. Solving the optimal control problem for u, that is for the minimum variation (optimal) control input that achieves elimination of the state vector's tracking error, we obtain $u = -\frac{1}{r}B^T Pe$.

Equivalently, solving the optimal control problem for $\tilde{d}$, that is for the worst case disturbance that the control loop can sustain, we obtain $\tilde{d} = \frac{1}{\rho^2}L^T Pe$.

The diagram of the considered control loop for the system of the integrated system that comprises a gas compressor driven by a 5-phase IM is depicted in Figure 3.
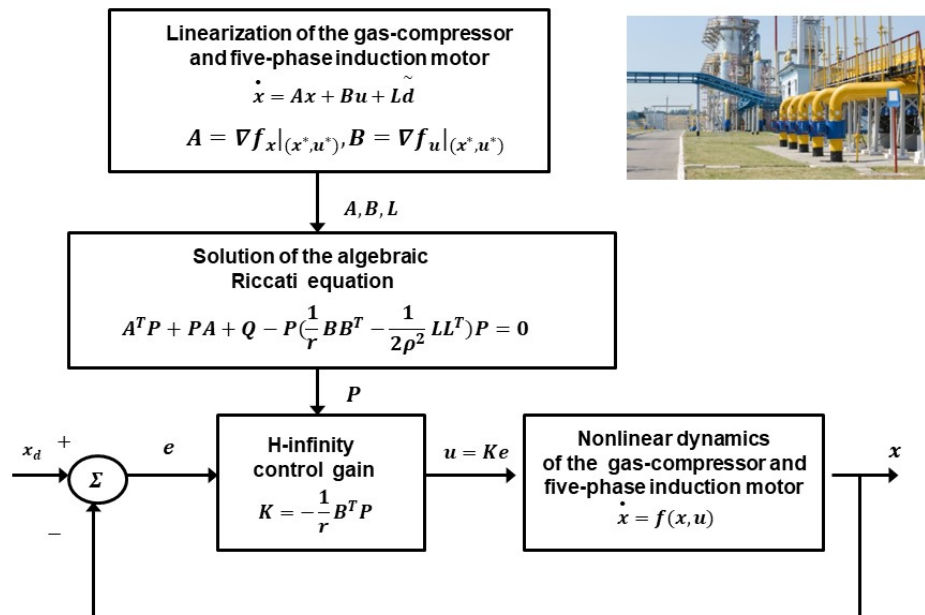

Fig. 3. Diagram of the control scheme for the integrated system of the gas compressor driven by a 5-phase IM. 5-phase IM, five-phase induction motor. Authors' own work.

Remark 1: Comparing to other nonlinear control methods that one could have considered for the gas compressor that is driven by the 5-phase IM, the presented nonlinear optimal (H-infinity) control approach exhibits specific advantages.

(a) In comparison to global linearisation-based control schemes (such as Lie-algebra-based control and flatness-based control), the nonlinear optimal control approach does not make use of complicated changes of state variables (diffeomorphims) and transformations of the system's state-space description. The computed control inputs are applied directly on the initial nonlinear state-space model of the gas compressor that is driven by the 5-phase IM without the intervention of inverse transformations and thus without coming against the risk of singularities.

(b) In comparison to NMPC and to classical MPC, the global stability properties of the nonlinear optimal control method are ensured. It is known that the performance and convergence to optimum of the iterative search of NMPC depends on parameter values' selection and on initialisation (multiple shooting methods).

(c) It is noteworthy that the use of the nonlinear optimal control method is not constrained to dynamical systems that have a specific state-space form (input–output-linearised, canonical, strict-feedback, or other). For instance, in sliding-mode control, unless the system is written in the input–output linearised form, there is no systematic procedure for defining sliding surfaces. Moreover, in backstepping control, unless the system is found in the strict-feedback (backstepping integral) form, there is no standard procedure for computing the backstepping control signal.

(d) In comparison to PID-type control, the nonlinear optimal control method is of proven global stability, does not rely on any heuristics for selecting the controller's feedback gains, and has global stability properties that are not affected by any changes in the operating points. It is known that the performance of PID (Proportional Integral Derivative) controllers depends on empirical tuning, which is performed around local operating points.

(e) Unlike multiple models-based feedback control, the nonlinear optimal control method relies on the use of one single linearisation point and avoids the need for defining empirically multiple fixed points. It also needs to solve only one Riccati equation and does not come against the solution of LMIs (Linear Matrix Inequalities). Consequently, the nonlinear optimal control method does not come against dimensionality issues due to an exponential growth of the parameters of the control problem. As a consequence, the method's computational complexity remains moderate.

6. Lyapunov Stability Analysis

6.1. Stability proof

Through Lyapunov stability analysis, it will be shown that the proposed nonlinear control scheme assures H_∞ tracking performance for the system of the gas compressor that is driven by a 5-phase IM, and that in case of bounded disturbance terms asymptotic convergence to the reference setpoints is achieved. The tracking error dynamics for the gas compressor that is driven by the 5-phase IM is written in the form

$$\dot{e} = Ae + Bu + L\tilde{d} \tag{47}$$

where in the compressor and 5-phase IM motor case $L = \in R^{11\times11}$ is the disturbance inputs gain matrix. Variable $\tilde{d}$ denotes model uncertainties and external disturbances of the model of the gas-compression system. The following Lyapunov equation is considered (Rigatos, 2016; Rigatos and Karapanou, 2020):

$$V = \tfrac{1}{2}e^T Pe \tag{48}$$

where $e = x - x_d$ is the tracking error. By differentiating with respect to time, one obtains

$$\dot{V} = \tfrac{1}{2}\dot{e}^T Pe + \tfrac{1}{2}e^T P\dot{e} \Rightarrow$$
$$\dot{V} = \tfrac{1}{2}[Ae + Bu + L\tilde{d}]^T Pe + \tfrac{1}{2}e^T P[Ae + Bu + L\tilde{d}] \Rightarrow \tag{49}$$

$$\dot{V} = \tfrac{1}{2}[e^T A^T + u^T B^T + \tilde{d}^T L^T]Pe +$$
$$+ \tfrac{1}{2}e^T P[Ae + Bu + L\tilde{d}] \Rightarrow \tag{50}$$

$$\dot{V} = \tfrac{1}{2}e^T A^T Pe + \tfrac{1}{2}u^T B^T Pe + \tfrac{1}{2}\tilde{d}^T L^T Pe + \tfrac{1}{2}e^T PAe + \tfrac{1}{2}e^T PBu + \tfrac{1}{2}e^T PL\tilde{d} \tag{51}$$

The previous equation is rewritten as

$$\dot{V} = \tfrac{1}{2}e^T(A^T P + PA)e + (\tfrac{1}{2}u^T B^T Pe + \tfrac{1}{2}e^T PBu) + (\tfrac{1}{2}\tilde{d}^T L^T Pe + \tfrac{1}{2}e^T PL\tilde{d}) \tag{52}$$

Assumption: For a given positive definite matrix Q and coefficients r and ρ, there exists a positive definite matrix P, which is the solution of the following matrix equation:

$$A^T P + PA = -Q + P(\tfrac{2}{r}BB^T - \tfrac{1}{\rho^2}LL^T)P \tag{53}$$

Moreover, the following feedback control law is applied to the system:

$$u = -\tfrac{1}{r}B^T Pe \tag{54}$$

By substituting Eq. (53) and Eq. (54), one obtains

$$\dot{V} = \tfrac{1}{2}e^T[-Q + P(\tfrac{2}{r}BB^T - \tfrac{1}{\rho^2}LL^T)P]e + e^T PB(-\tfrac{1}{r}B^T Pe) + e^T PL\tilde{d} \Rightarrow \tag{55}$$

$$\dot{V} = -\tfrac{1}{2}e^T Qe + \tfrac{1}{r}e^T PBB^T Pe - \tfrac{1}{2\rho^2}e^T PLL^T Pe - \tfrac{1}{r}e^T PBB^T Pe + e^T PL\tilde{d} \tag{56}$$

which, after intermediate operations, gives

$$\dot{V} = -\tfrac{1}{2}e^T Qe - \tfrac{1}{2\rho^2}e^T PLL^T Pe + e^T PL\tilde{d} \tag{57}$$

or, equivalently,

$$\dot{V} = -\tfrac{1}{2}e^T Qe - \tfrac{1}{2\rho^2}e^T PLL^T Pe + \tfrac{1}{2}e^T PL\tilde{d} + \tfrac{1}{2}\tilde{d}^T L^T Pe \tag{58}$$

Lemma: The following inequality holds

$$\tfrac{1}{2}e^T PL\tilde{d} + \tfrac{1}{2}\tilde{d}L^T Pe - \tfrac{1}{2\rho^2}e^T PLL^T Pe \leq \tfrac{1}{2}\rho^2 \tilde{d}^T \tilde{d} \tag{59}$$

Proof: The binomial $(\rho\alpha - \tfrac{1}{\rho}b)^2$ is considered. Expanding the left part of the above inequality, one obtains

$$\rho^2 a^2 + \tfrac{1}{\rho^2}b^2 - 2ab \geq 0 \Rightarrow \tfrac{1}{2}\rho^2 a^2 + \tfrac{1}{2\rho^2}b^2 - ab \geq 0 \Rightarrow$$
$$ab - \tfrac{1}{2\rho^2}b^2 \leq \tfrac{1}{2}\rho^2 a^2 \Rightarrow \tfrac{1}{2}ab + \tfrac{1}{2}ab - \tfrac{1}{2\rho^2}b^2 \leq \tfrac{1}{2}\rho^2 a^2 \tag{60}$$

The following substitutions are carried out: $a = \tilde{d}$ and $b = e^T PL$; and the previous relation becomes

$$\tfrac{1}{2}\tilde{d}^T L^T Pe + \tfrac{1}{2}e^T PL\tilde{d} - \tfrac{1}{2\rho^2}e^T PLL^T Pe \leq \tfrac{1}{2}\rho^2 \tilde{d}^T \tilde{d} \tag{61}$$

Eq. (61) is substituted in Eq. (58) and the inequality is enforced, thus giving

$$\dot{V} \leq -\tfrac{1}{2}e^T Qe + \tfrac{1}{2}\rho^2 \tilde{d}^T \tilde{d} \tag{62}$$

Eq. (62) shows that the H_∞ tracking performance criterion is satisfied. The integration of V from 0 to T gives

$$\int_0^T \dot{V}(t)dt \leq -\frac{1}{2}\int_0^T ||e||_Q^2 dt + \frac{1}{2}\rho^2 \int_0^T ||\tilde{d}||^2 dt \Rightarrow$$
$$2V(T) + \int_0^T ||e||_Q^2 dt \leq 2V(0) + \rho^2 \int_0^T ||\tilde{d}||^2 dt \tag{63}$$

Moreover, if there exists a positive constant $M_d > 0$ such that

$$\int_0^\infty ||\tilde{d}||^2 dt \leq M_d \tag{64}$$

then one obtains

$$\int_0^\infty ||e||_Q^2 dt \leq 2V(0) + \rho^2 M_d \tag{65}$$

Thus, the integral $\int_0^\infty ||e||_Q^2 dt$ is bounded. Moreover, $V(T)$ is bounded and from the definition of the Lyapunov function V in Eq. (48) it becomes clear that $e(t)$ will be also bounded since $e(t) \in \Omega_e = \{e|e^T Pe \leq 2V(0) + \rho^2 M_d\}$. According to the above and with the use of Barbalat's lemma, one obtains $\lim_{t \to \infty} e(t) = 0$.

After following the stages of the stability proof, one arrives at Eq. (62), which shows that the H-infinity tracking performance criterion holds. By selecting the attenuation coefficient ρ to be sufficiently small and in particular to satisfy $\rho^2 < ||e||_Q^2/||\tilde{d}||^2$, one has that the first derivative of the Lyapunov function is upper bounded by 0. This condition holds at each sampling instance and consequently global stability for the control loop can be concluded.

6.2. Robust state estimation with the use of the H$_\infty$ Kalman filter

The control loop has to be implemented with the use of information provided by a small number of sensors and by processing only a small number of state variables. To reconstruct the missing information about the state vector of the system of the gas compressor that is driven by a 5-phase IM, it is proposed to use a filtering scheme and, based on it, to apply state estimation-based control (Rigatos, 2015, 2016). By denoting as $A(k)$, $B(k)$, and $C(k)$ the discrete-time equivalents of matrices A, B, and C of the linearised state-space model of the system, the recursion of the H_∞ Kalman filter for the model of the electrically actuated compressors' system can be formulated in terms of a *measurement update* and a *time update* parts.

Measurement update:

$$D(k) = [I - \theta W(k)P^-(k) + C^T(k)R(k)^{-1}C(k)P^-(k)]^{-1}$$
$$K(k) = P^-(k)D(k)C^T(k)R(k)^{-1} \tag{66}$$

$$\hat{x}(k) = \hat{x}^-(k) + K(k)[y(k) - C\hat{x}^-(k)]$$

Time update:

$$\hat{x}^-(k+1) = A(k)x(k) + B(k)u(k)$$
$$P^-(k+1) = A(k)P^-(k)D(k)A^T(k) + Q(k) \tag{67}$$

where it is assumed that parameter θ is sufficiently small to assure that the covariance matrix $P^-(k)^{-1} - \theta W(k) + C^T(k) R(k)^{-1}C(k)$ will be a positive definite. When $\theta = 0$, the H_∞ Kalman filter becomes equivalent to the standard Kalman filter. One can measure only a part of the state vector of the system of the 5-phase IM-driven gas compressor, and can estimate through filtering the rest of the state vector elements that are associated with the turn speed of the compressor or with magnetic flux variables of the stator of the 5-phase IM. Moreover, the proposed Kalman filtering method can be used for sensor fusion purposes.

7. Simulation Tests

To test the performance of the proposed nonlinear optimal control method, simulation experiments have been carried out. To implement the nonlinear optimal control method, the algebraic Riccati equation of Eq. (53) had to

be solved at each sampling period with the use of Matlab's *aresolv()* function. It has been confirmed that the time-interval that is needed for solving this Riccati equation is significantly smaller than the sampling period, which was $T_s = 0.01$ s. Indicative values about the parameters of the 5-phase IM-driven gas compressor have been as follows: (a) gas compressor: $a_i = 1.5$, $V_i = 10.2$ m³, $a_0 = 4.5$, $V_o = 4.0$ m^3, $p_{atm} = 1.1$ atm, $K_o = 0.1$, $L = 1.0$, and $v = 0.01$; (b) 5-phase IM: $P = 4$, $J = 2.0$ kg·m^2, $R_s = 0.16\Omega$, $R_r = 0.10\Omega$, $L_s = 20.4$mH, $L_r = 20.3$ mH $M = 6.4$ mH, and $L_{1s} = 0.1$ mH. To implement state estimation-based control, the H-infinity Kalman filter has been used as a robust state estimator. The obtained results come from three different simulation tests (each test is associated with different setpoints) and are depicted in Figures 4–9. The state variables' values are normalised and presented in a per-unit system. The real values of the
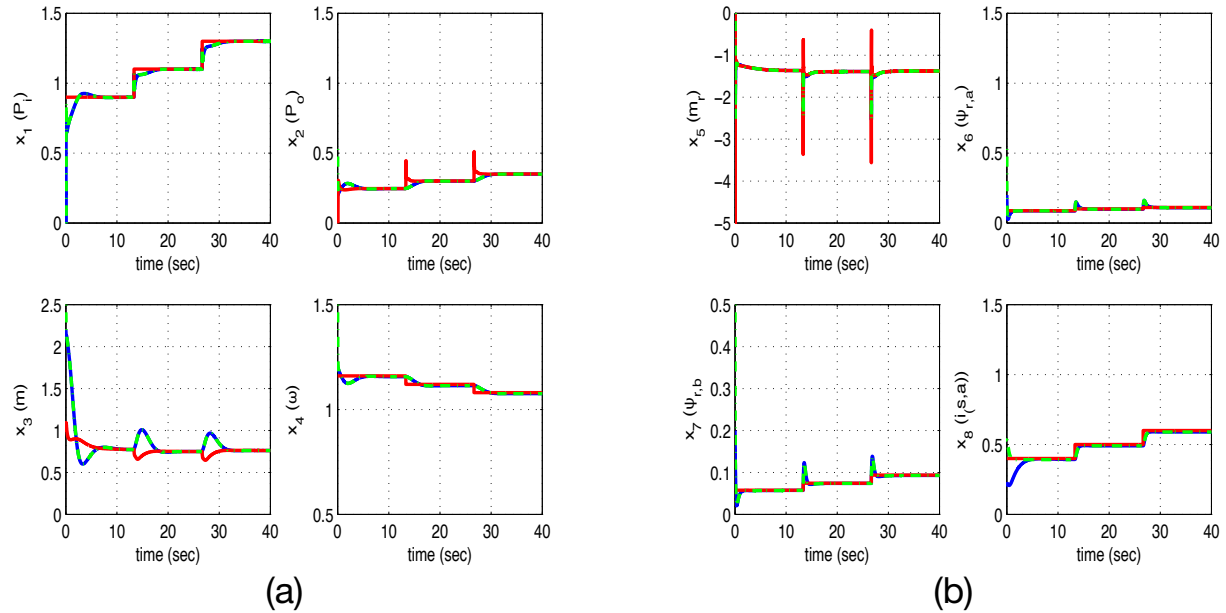

Fig. 4. Tracking of setpoint 1 for the gas compressor that is driven by a 5-phase IM: (a) convergence of state variables x_1 to x_4 to their reference setpoints (red line: setpoint, blue line: real value, green line: estimated value), (b) convergence of state variables x_5 to x_8 to their reference setpoints (red line: setpoint, blue line: real value, green line: estimated value). Authors' own work.
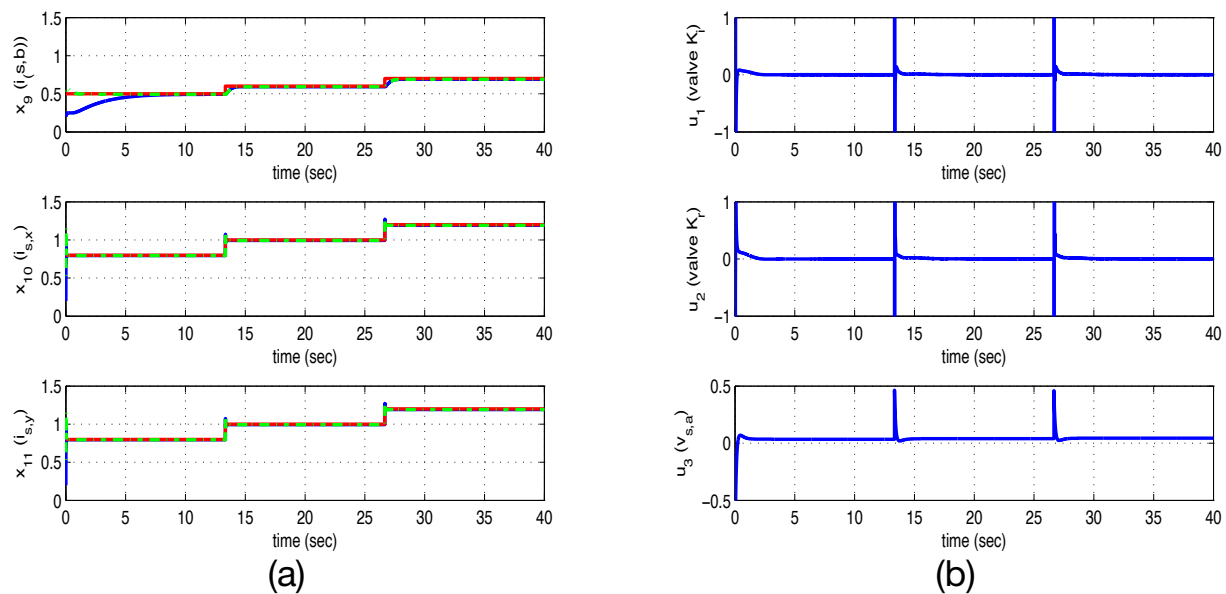

Fig. 5. Tracking of setpoint 1 for the gas compressor that is driven by a 5-phase IM: (a) convergence of state variables x_9 to x_{11} to their reference setpoints (red line: setpoint, blue line: real value, green line: estimated value), (b) control inputs u_1 to u_3. Authors' own work.
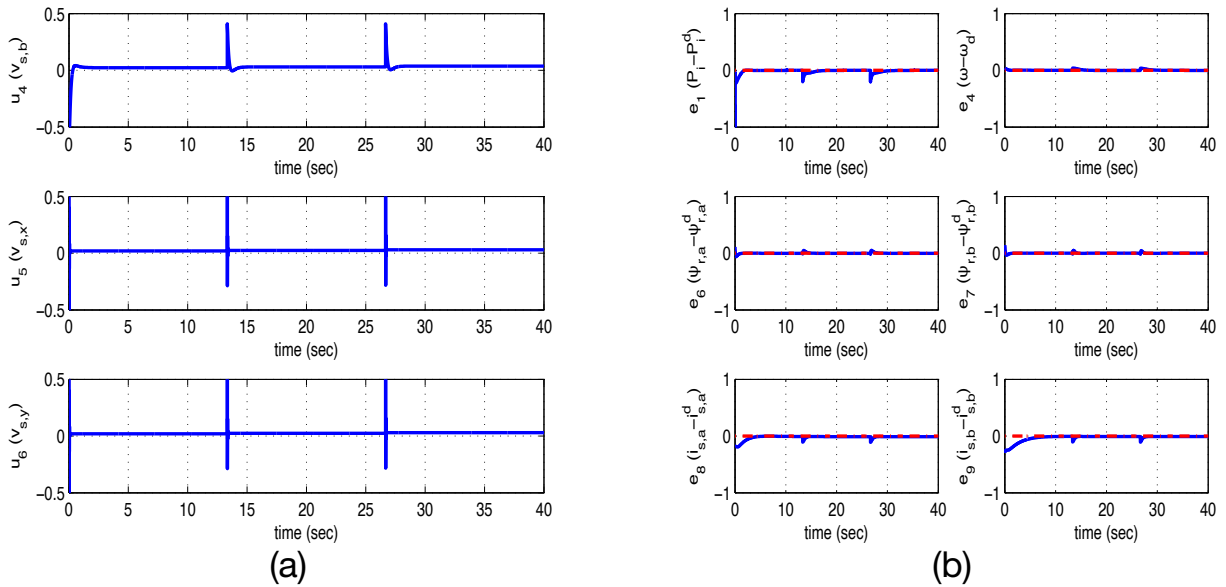
Fig. 6. Tracking of setpoint 1 for the gas compressor that is driven by a 5-phase IM: (a) control inputs u_4 to u_6, (b) convergence to zero of the tracking error for the indicative state variables of the gas-compression system. Authors' own work.
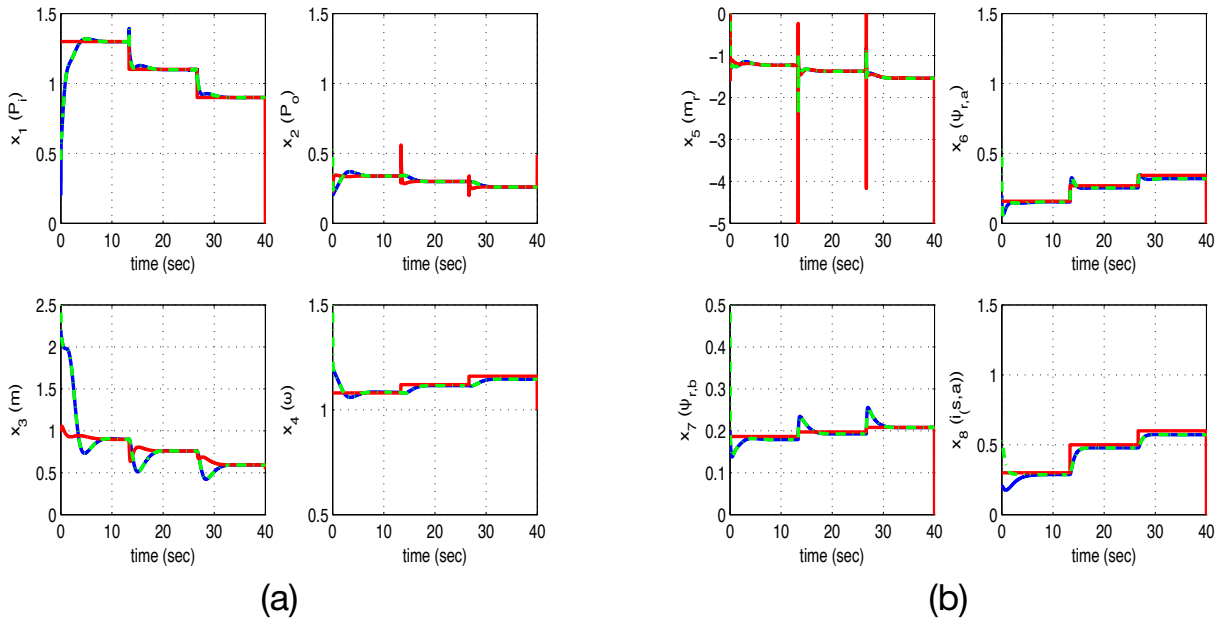

Fig. 7. Tracking of setpoint 2 for the gas compressor that is driven by a 5-phase IM: (a) convergence of state variables x_1 to x_4 to their reference setpoints (red line: setpoint, blue line: real value, green line: estimated value), (b) convergence of state variables x_5 to x_8 to their reference setpoints (red line: setpoint, blue line: real value, green line: estimated value). Authors' own work.

state variables of the integrated gas-compression system are shown in blue colour and the associated setpoints are depicted in red, whereas the estimated values that are provided by the H-infinity Kalman filter are plotted in green. Through the simulation experiments, it has been confirmed that the nonlinear optimal control approach achieves fast and accurate tracking of setpoints by the state variables of the 5-phase IM-driven gas compressors under
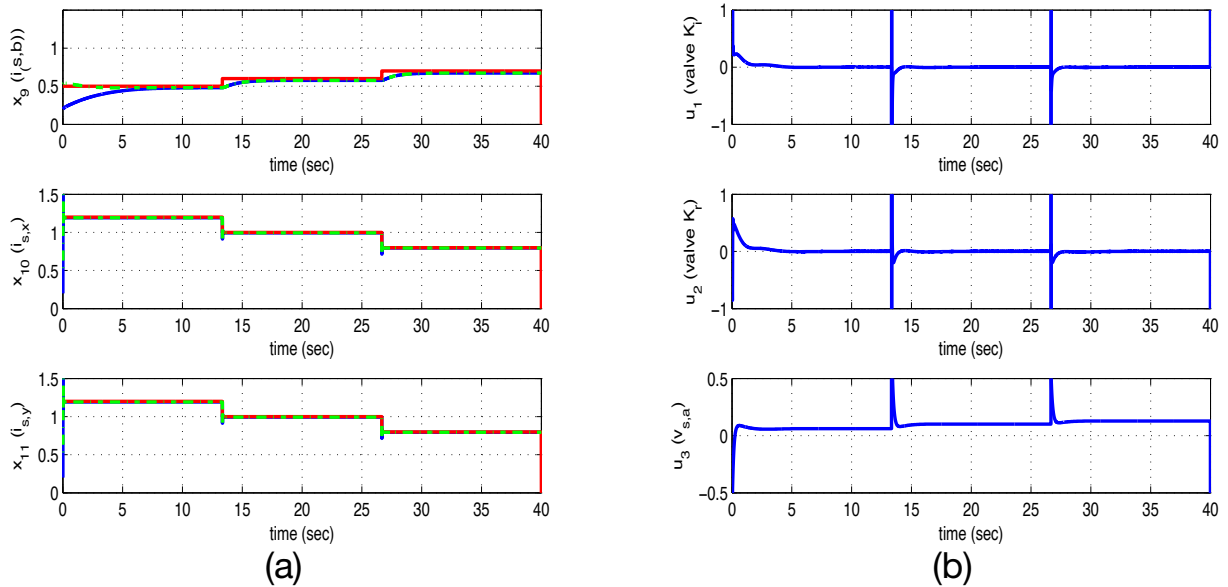
Fig. 8. Tracking of setpoint 2 for the gas compressor that is driven by a 5-phase IM: (a) convergence of state variables x_9 to x_{11} to their reference setpoints (red line: setpoint, blue line: real value, green line: estimated value), (b) control inputs u_1 to u_3. Authors' own work.
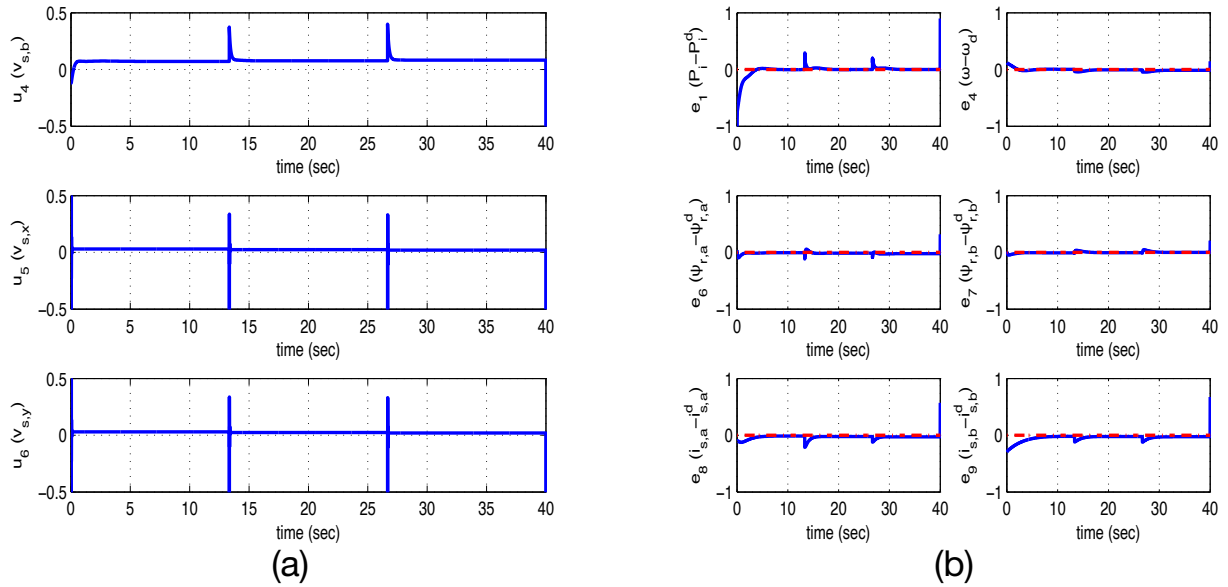

Fig. 9. Tracking of setpoint 2 for the gas compressor that is driven by a 5-phase IM: (a) control inputs u_4 to u_6, (b) convergence to zero of the tracking error for the indicative state variables of the gas-compression system. Authors' own work.

moderate variations of the control inputs. The variations of the Lyapunov function of the control system of the gas compressor and the 5-phase IM are also shown in the diagrams given in Figure 10. The global stability properties of the nonlinear optimal control method are confirmed once again. Finally, using the inverse of the Clarke's/Park's transformation matrix of Eq. (6), the diagrams of Figure 11 have been obtained, depicting the variation of the phase currents of 5-phase IM.
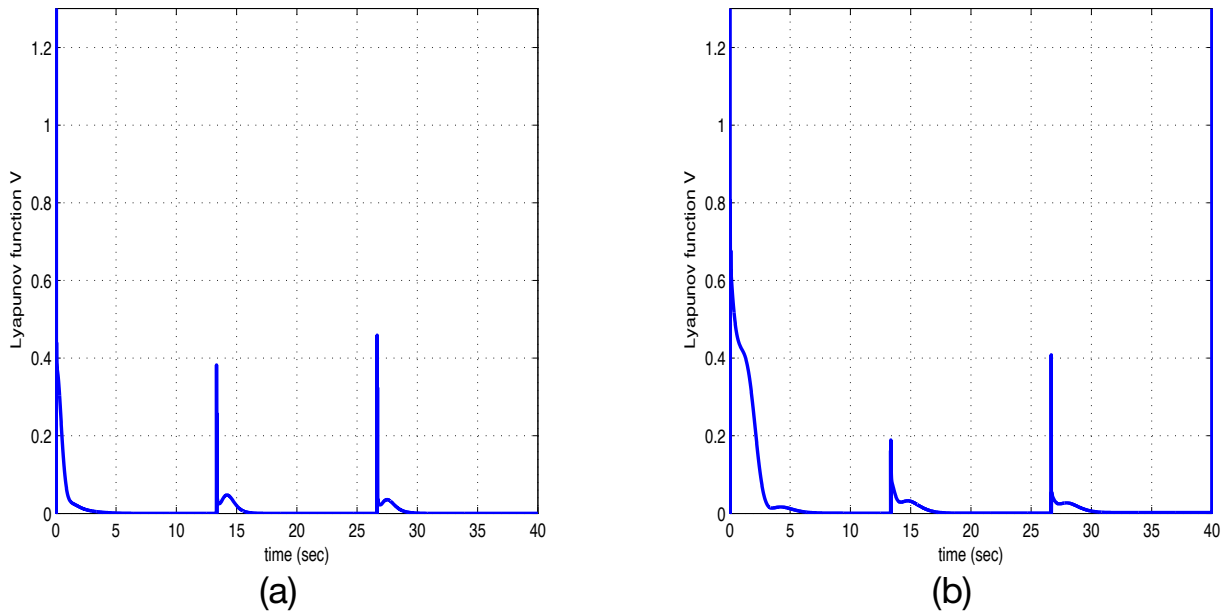
Fig. 10. Variation of the Lyapunov function of the control system of the gas compressor and of the 5-phase IM: (a) when tracking setpoint 1, (b) when tracking setpoint 2. Authors' own work.
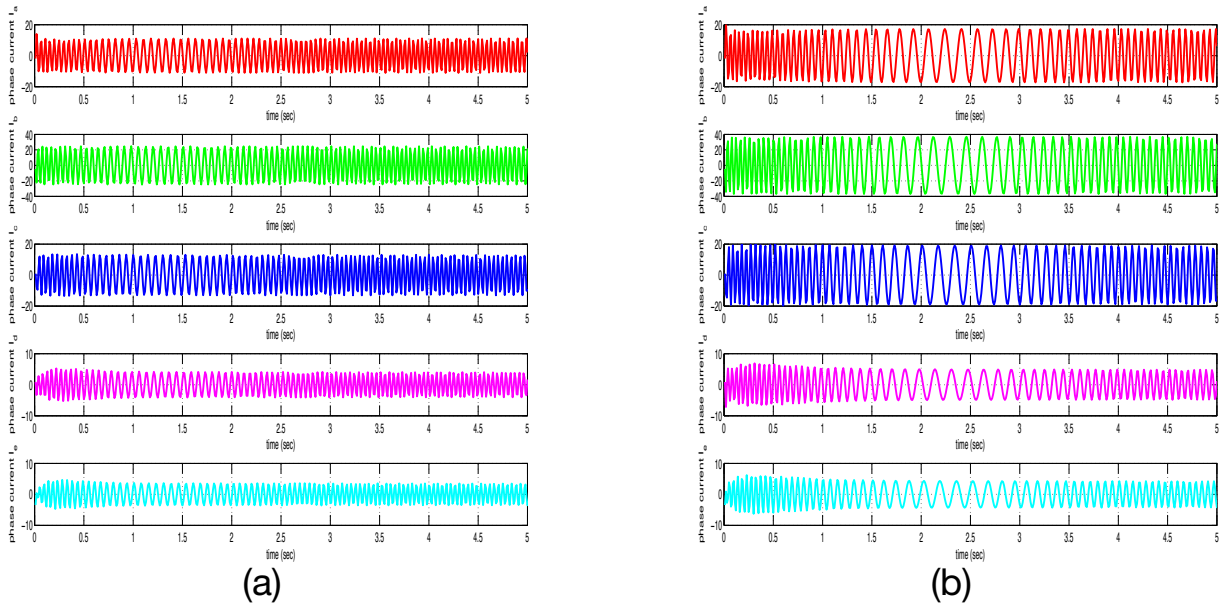

Fig. 11. Variation of the phase currents of the 5-phase IM: (a) when tracking setpoint 1, (b) when tracking setpoint 2. Authors' own work.

To elaborate on the above-noted diagrams and on the fine tracking performance and the global stability properties of the nonlinear optimal control method for the electrically actuated gas compressor, the following tables are also provided: (i) Table 1 providing data about the accuracy of tracking of setpoints by the state variables of the gas compression system under an exact dynamic model, (ii) Table 2 providing data about the accuracy of state estimation that is achieved by the H-infinity Kalman filter, and (iii) Table 3 providing data about the speed of convergence of the state variables of the gas compression system to the targeted setpoints.

No test	RMSE$_{x1}$	RMSE$_{x2}$	RMSE$_{x3}$	RMSE$_{x4}$	RMSE$_{x5}$	RMSE$_{x6}$	RMSE$_{x7}$	RMSE$_{x8}$	RMSE$_{x10}$
Test$_1$	0.0506	0.0263	0.0320	0.1875	0.0287	0.1320	0.0219	0.5095	0.3467
Test$_2$	0.0508	0.0253	0.0377	0.1726	0.0335	0.1284	0.0247	0.5095	0.3467

Table 1. Tracking RMSE (Root Mean Square Error) for the 5-phase IM-driven gas compressor in the disturbance-free case $\times 10^{-3}$
5-phase IM, five-phase induction motor.

No test	RMSE$_{x1}$	RMSE$_{x2}$	RMSE$_{x3}$	RMSE$_{x4}$	RMSE$_{x5}$	RMSE$_{x6}$	RMSE$_{x7}$	RMSE$_{x8}$	RMSE$_{x}$10
Test$_1$	0.2518	0.2384	0.2607	0.2419	0.2636	0.2426	0.2578	0.0275	0.2379
Test$_2$	0.2491	0.2572	0.2636	0.2446	0.2611	0.2565	0.2486	0.0498	0.2682

Table 2. Estimation RMSE for the H-infinity Kalman filter $\times 10^{-6}$

No test	$T_s x1$	$T_s x2$	$T_s x3$	$T_s x4$	$T_s x5$	$T_s x6$	$T_s x7$	$T_s x8$	$T_s x10$
Test$_1$	6.0	5.0	6.0	5.0	0.5	1.0	1.0	6.0	0.5
Test$_2$	7.0	7.0	8.5	7.0	0.5	1.0	1.0	6.0	0.5

Table 3. Convergence times (sec) for the 5-phase IM-driven gas compressor
5-phase IM, five-phase induction motor.

8. Conclusions

The article has addressed the nonlinear optimal control problem for the integrated gas-compression system that comprises a gas compressor that is actuated by a 5-phase IM. First, the state-space model of the integrated gas-compression system has undergone approximate linearisation with the use of first-order Taylor series expansion and through computation of the associated Jacobian matrices. The linearisation process is repeated at each sampling instance around a temporary operating point that is defined by the present value of the system's state vector and by the last sampled value of the control inputs vector. For the linearised model of the system, a stabilising H-infinity feedback controller is designed. To select the controller's gains, an algebraic Riccati equation is repetitively solved at each iteration of the control algorithm. The global stability properties of the control scheme are proven through Lyapunov analysis. To implement state estimation-based control without the need to measure the entire state vector of the gas-compression system, the H-infinity Kalman filter has been used as a robust state estimator.

The proposed nonlinear optimal control method exhibits specific advantages in comparison to other nonlinear control schemes one could have considered for the dynamic model of a centrifugal gas compressor with actuation from a 5-phase IM. Unlike global linearisation-based control schemes, as for instance Lie-algebra-based control, the nonlinear optimal control method avoids complicated transformations of state-space descriptions and changes of state variables and does not come against singularity issues. Unlike nonlinear model-predictive control schemes, the nonlinear optimal control method is of proven global stability. Unlike sliding-mode control and backstepping control approaches, the application of the nonlinear optimal control method does not have as a prerequisite the state-space model of the system to be found into a specific form (for instance the input–output linearised or the triangular form). Unlike PID control schemes, the nonlinear optimal control method is of ensured global stability and the selection of the gains of the optimal controller is not based on heuristics. Finally, it is noted that the use of 5-phase IMs for the actuation of gas compressors is also advantageous, because it achieves higher power and torque rates, smoother distribution of power to the phases of the motor, less stressing of the associated voltage inverters, and fault tolerance in the case of failure of one or more phases.

Statement of conflict disclosure

The authors of this article state that, to their knowledge, no conflict of interest exists with third parties or other members of the scientific community about the content and results of the present research.

Data availability

The authors of this article state that data associated with the experimental results of the research can be made available upon reasonable request.

References

Arahal, M. R., Duran, M. J., Barrero, F. and Toral, S. (2010). Stability Analysis of Five-Phase Induction Motor Drives with Variable Third Harmonic Injection. *Electric Power Systems Research*. 80, pp. 1459–1468.

Arahal, M. R., Martin, C., Kowal, A., Castillo, M. and Barrero, F. (2020a). Cost Function Optimization for Predictive Control of A Five-Phase IM. *Optimal Control Applications and Methods*, 41(1), pp. 84-93.

Arahal, M. R., Martin, C., Barrero, F. and Duran, M. J. (2020b). Assessing Variable Sampling Time Controllers for Five-Phase Induction Motor Drives. *IEEE Transactions on Industrial Electronics*, 67(4), pp. 2523–2532.

Arashloo, R. S., Salehifar, M., Romeral, L. and Sala, V. (2019). A Robust Predictive Current Controller for Healthy and Open Circuit Faulty Condition of Five-Phase BLDC Drives Applicable for Wind Generators and Electric Vehicles. *Energy Conversion and Management*, 92(1), pp. 437–447.

Basseville, M., and Nikiforov, I. (1993). *Detection of Abrupt Changes: Theory and Applications*, Prentice-Hall.

Behegen, B., and Gravdahl, T.M. (2008). Active Surge Control of Compression System Using Drive Torque. *Automatica*, 44(4), 1135–1140.

Bernudes, M., Martin, C., Gonzalez-Prieto, I., Duran, M. J., Arahal, M. R. and Barrero, F. (2020). Predictive Current Control in Electrical Drives: An Illustrative Review with Case Examples Using A Five-Phase Induction Motor with Drive Distributed Winding. *IET Electic Power Applications*, 14(8), 1291–1310.

Budinis, S. and Thornhill, M. F. (2018). Control of centrifugal compressors via model predictive control for enhanced oil recovery applications. In: *IFAC 2nd Workshop on Automatic Control of Offshore Oil and Gas Production*, Florianapolis, Brazil.

Durantay, L., Gelin, A., Thibaut, E. and Vidalenc, Y. (2019a), Integrated moto-compressor versus conventional solution. In: *IEEE PCIC 2019, IEEE Petroleum and Chemical Industry Conference*, Paris, France, May 2019.

Durantay, L., Alban, T., Siala, S. and Billaud, A. (2019b), Selection and Tests of Innovative Variable-Speed Motor-Compressor Solutions for A 55MW Full Electric Offshore Platform Maximizing Availability and Efficiency with Better Environmental Impact. *IEEE Transactions on Industry Applications*, 55(6), pp. 6678–6689.

Echeich, M., Trabelsi, R., Kesraoui, H., Iqbal, A. and Mimouni, M. F. (2020). Torque Ripple Improvement of Direct Torque Controlled Five-Phase Induction Motor Drive Using Backstepping Control. *International Journal of Power Electronics and Drive Systems*, 11(1), pp. 64–74.

Echeikh, H., Trabelsi, R., Iqbal, A. and Mimouni, M. R. (2018). Real-Time Implementation of Indirect Rotor Flux Oriented Control of A Five-Phase Induction Motor with Novel Rotor Resistance Adaptation Using Sliding-Mode Observer. *Journal of the Franklin Institute*, 335(5), pp. 2112–2141.

Echeikh, M., Trabelsi, R., Iqbal, A., Bianchi, N. and Mimouni, M. F.(2016). Comparative Study Between the Rotor Flux Oriented Control and Nonlinear Backstepping Control of A Five-Phase Induction Motor Drive an Experimental Validation. *IET Power Electronics*, 9(3), pp. 2510–2521.

Gonzalez-Prieto, L., Duran, M. J., Rios-Garcia, N., Barrera, F. and Martin, C. (2018). Open-Switch Fault Detection in Five-Phase Induction Motor Drives Using Model-Predictive Control. *IEEE Transactions on Industrial Electronics*, 65(4), pp. 3045–3055.

Gravdahl, J. T., Egeland, O. and Vatland, S. O. (2002). Drive Torque Actuation in Active Surge Control of Centrifugal Compressors. *Automatica*, 38(11), pp. 1881–1893.

Han, X., Liu, C., Chen, B. and Zhang, S. (2022). Surge Disturbance Suppression of AMB-Rotor Systems in Magnetically Suspended Centrifugal Compressors. *IEEE Transactions on Control Systems Technology*, 30(4), pp. 1550–1560.

Khadar, S., Abu-Rub, H. and Kouzou, A. (2021). Sensorless Field-Oriented Control for Open-End Winding Five-Phase Induction Motor with Parameters Estimation. *IEEE Open Access Journal of the Industrial Electronics Society*, 2, pp. 265–278.

Li, T., Ma, R. and Han, W. (2020). Virtual Vector-Based Model Predictive Current Control of Five-Phase PMSM with Stator Current and Concentrated Disturbance Observer. *IEEE Access*, 8, pp. 212635–212646.

Lu, Y., Wang, P., Jin, M. and Qi, Y. (2016). Centrifugal Compressor Fault Diagnosis Based on Qualitative Simulation and Thermal Parameters. *Mechanical Systems and Signal Processing*, 81, pp. 253–273.

Ma, X., Zhang, S. and Wang, K. (2019). Active Surge Control for Magnetically Suspended Centrifugal Compresors Using A Variable Equilibrium Point Approach. *IEEE Transactions on Industrial Electronics*, 66(12), pp. 9363–9393.

Martin, C., Arahal, M. R., Barrera, F. and Duran, M. J. (2016). Five-Phase Induction Motor Rotor Current Observer for Finite Control Set Model Predictive Control of Stator Current. *IEEE Transactions on Industrial Electronics*, 63(7), pp. 4527–4538.

Mochammad, S., Kong, Y. J., Noh, Y., Park, S. and Ahn, B. (2021). Stable hybrid feature selection method for compressor fault diagnosis. *IEEE Access*, 9: pp. 97415–97429.

Morawiec, M. and Wilczynski, F. (2022). Srrong Strategy of A Five-Phase Induction Machine Supplied by the Current Source Inverter with the Third Harmonic Injection. *IEEE Transactions on Power Electronics*, 37(8), pp. 9539–9550.

Morawiec, M., Stranlowkski, P., Lewicki, A., Guzinski, J. and Wilczynski, F. (2020). Feedback Control of Multiphase Induction Machines with Backstepping Techniques. *IEEE Transactions on Industrial Electronics*, 67(6), pp. 4305–4314.

Priestley, M., Fletcher, J. E. and Tan, C. (2018). Space-Vector PWM Technique for Five-Phase Open-End Winding PMSM Drive Operating in the Overmodulation Region. *IEEE Transactions on Industrial Electronics*, 65(9), pp. 6816–6827.

Rigatos. G, (2016). *Intelligent Renewable Energy Systems: Modelling and Control*. Springer.

Rigatos, G. (2011). *Modelling and Control for Intelligent Industrial Systems: Adaptive Algorithms in Robotics and Industrial Engineering*. Springer.

Rigatos, G. (2015). *Nonlinear Control and Filtering Using Differential Flatness Approaches: Applications to Electromechanical Systems*. Springer.

Rigatos, G. and Karapanou, E. (2020). *Advances in Applied Nonlinear Optimal Control*. Cambridge Scholars Publishing.

Rigatos, G., and Zhang, Q. (2009). Fuzzy Model Validation Using the Local Statistical Approach. *Fuzzy Sets and Systems*, 60(7), pp. 882–904.

Rigatos, G., Abbaszadeh, M. and Siano, P (2022). *Control of Dynamical Nonlinear and Partial Differential Equation Systems: Theory and Applications*. IET Publications.

Rigatos, G. G. and Tzafestas, S. G. (2007). Extended Kalman Filtering for Fuzzy Modelling and Multi-Sensor Fusion. *Mathematical and Computer Modelling of Dynamical Systems, Taylor & Francis*, 13(3), pp. 251–266.

Riveros, J. A., Barrero, F., Levi, E., Duran, M. J., Toral, S. and Jones, M. (2018). Variable-Speed Five-Phase Induction Motor Drive Based on Predictive Torque Control. *IEEE Transactions on Industrial Electronics*, 60(8), pp. 2957–2968.

Saad, K., Abdellah, K., Ahmed, H. and Iqbal, A. (2019). Investigation of SVM-Backstepping Sensorless Control of Five-Phase Open-End Winding Induction Motor Based on Model Reference Adaptive System and Parameter Estimation. *Engineering Science and Technology*, 22(4), pp. 1013–1026.

Singhal, S. (2014). Electric Drive Compressor Systems: High-Speed Turbo Compressors Used in the Oil and Gas Industry. *IEEE Industry Applications Magazine*, 20(6), pp. 52–63.

Soleymani, R., Nekani, M. A. and Mourefianpour, M. (2019). A Novel Robust Fault Detection Method for Induction Motor Rotor by Using Unknown Input Observer. *Systems Science and Control Engineering*, 7(1), pp. 109–115.

Tessarolo, A., Ziocco, G. and Tonello, C. (2011), Design and Testing of a 45MW 100Hz Quadruple-Star Synchronous Motor for A Liquified Natural Gas Turbo Compressor Drive. *IEEE Transactions on Industry Applications*, 47(3), pp. 1210–1219.

Torrisi, G., Jaramillo, V., Ottewill, J. R., Mariethoz, M., Morari, M. and Smith, R. S. (2015). Active Surge Control of Electrically Driven Cntrifugal Compressors. In: *2015 European Control Conference*, Linz, Austria.

Torrissi, G., Grammatico, S., Cortinovis, M., Mercangoz, M., Morari, M. and Smith, R. S. (2019). Model Predictive Approaches for Active Surge Control in Centrifugal Compressors. *IEEE Transactions on Control Systems Technology*, 29(6), pp. 1947–1960.

Toussaint, G. J., Basar, T. and Bullo, F. (2000), H_∞ Optimal Tracking Control Techniques for Nonlinear Underactuated Systems. In: *Proceedings of the 39th IEEE Conference on Decision and Control (IEEE CDC 2000)*, Sydney Australia, 12–15 December 2000.

Tribelsi, M. and Semail, E. (2021). Virtual Current Vector-Based Method for Inverter Open-Switch and Openphase Fault Diagnosis in Multi-Phase Permanent Magnet Synchronous Motor Drives. *IET Electric Power Applications*, 16(2), pp. 1476–1491.

Verma, M., Parker, D., Grindbaum, F. and Nanney, J. (2017). Making the Leap to Electric Motors and Adjustable Speed Drives: Case-Study of the 20000Hp Gas-Turbine-Driven Compressor. *IEEE Industry Applications Magazine*, 23(6), pp. 29–38

Xiang, S. and Li, J. (2022). Cascade Model Predictive Current Control for Five-Phase Permanent Magnet Synchronous Motor. *IEEE Access*, 10, pp. 88812–88820.

Xiong, C., Xu, H., Guan, T. and Zhou, P. (2020). A Constraint Switching Frequency Multiple-Vector-Based Model Predictive Current Control of Five-Phase PMSM with Nonsinusoidal Back EMF. *IEEE Transactions on Industrial Electronics*, 67(3), pp. 695–1707.

Zhou, Y., Yan, Z., Duan, Q., Wang, L. and Wu, X. (2019). Direct Torque Control Strategy of Five-Phase PMSM with Load Capacity Enhancement. *IET Power Electronics*, 12(3), pp. 598–606.